

Pachner moves in a 4d Riemannian holomorphic Spin Foam model

Andrzej Banburski,^{1,2} Lin-Qing Chen,^{1,2} Laurent Freidel,¹ and Jeff Hnybida³

¹ *Perimeter Institute for Theoretical Physics, Waterloo, Ontario, Canada.*

² *Department of Physics, University of Waterloo, Waterloo, Ontario, Canada*

³ *Institute for Mathematics, Astrophysics, and Particle Physics Faculty of Science,
Radboud University, Nijmegen, Netherlands*

In this work we study a Spin Foam model for 4d Riemannian gravity, and propose a new way of imposing the simplicity constraints that uses the recently developed holomorphic representation. Using the power of the holomorphic integration techniques, and with the introduction of two new tools: the homogeneity map and the loop identity, for the first time we give the analytic expressions for the behaviour of the Spin Foam amplitudes under 4-dimensional Pachner moves. It turns out that this behaviour is controlled by an insertion of nonlocal mixing operators. In the case of the 5–1 move, the expression governing the change of the amplitude can be interpreted as a vertex renormalisation equation. We find a natural truncation scheme that allows us to get an invariance up to an overall factor for the 4–2 and 5–1 moves, but not for the 3–3 move. The study of the divergences shows that there is a range of parameter space for which the 4–2 move is finite while the 5–1 move diverges. This opens up the possibility to recover diffeomorphism invariance in the continuum limit of Spin Foam models for 4D Quantum Gravity.

Contents

I. Introduction	2
II. Holomorphic Spin Foam Models	4
A. BF theory and Cable Diagrams	4
B. The Holomorphic Representation and Diagrammatics	6
C. Holomorphic Simplicity Constraints	8
D. Imposing constraints	9
1. DL prescription	10
2. Constrained projector	10
E. The Homogeneity Map	12
III. Pachner moves in 3d quantum gravity	14
A. Definition of Pachner Moves	14
B. Fixing the gauge	15
C. The Loop Identity	16
D. Alternative method	17
E. Invariance under Pachner moves and symmetry	18
1. 3–2 move	18
2. 4–1 move	18
IV. Pachner moves in 4d Riemannian holomorphic Spin Foam Model	20
A. Toy Loop	20
B. The Constrained Loop Identity	21
C. Computing Pachner Moves with Simplicity Constraints	23
1. 3–3 move	24
2. 4–2 move	27

3. 5–1 move	29
V. Towards coarse graining	32
A. Truncation of the loop identity	33
B. Counting the degree of divergence	35
C. Truncated Pachner moves	39
VI. Discussion	40
Acknowledgments	41
A. Gaussian Integration Techniques	41
B. Mapping $SU(2)$ to spinors	42
C. Group averaging the $SU(2)$ projector	43
D. Proof of Lemma (III.2)	43
E. Explicit calculation of the Constrained Loop Identity	44
References	45

I. INTRODUCTION

Spin Foam models attempt to rigorously define a path integral for transition amplitudes in Quantum Gravity [1, 2]. These models are well defined thanks to a discrete regularization of spacetime. The dynamics of this discrete structure is still not understood and is currently under intense investigation [3–6]. In this paper we study the Spin Foam dynamics for one particular model with the goal of determining its continuum limit. We also develop along the way new strategies, tools and techniques that can be applied to a larger class of models.

Spin Foam models for gravity are usually constructed in analogy with a formulation of General Relativity, due to Plebanski [7], as a constrained topological gauge theory known as BF theory. Each Spin Foam model is a proposal for a discretized version of these constraints, known as simplicity constraints. The most popular proposals are due to EPRL and FK [8–11]. In this paper we will focus on a Spin(4) Spin Foam model which is closely related to a model proposed by Dupuis and Livine [12], for 4d Riemannian Quantum Gravity. We choose this model because it is formulated in a holomorphic representation which is particularly suitable for performing analytical calculations.

The DL model arose from recent work in rewriting spin foams in a coherent state (or holomorphic) representation beginning with [13, 14] and leading to many new tools and interesting results [15–23]. In the holomorphic representation complicated integrals over $SU(2)$ group elements can be rewritten as simple integrals over the complex plane. This allows for exact evaluations of complicated spin network functions [24], and gives hope to study the dynamics of Spin Foam amplitudes analytically, and eventually numerically.

The natural path towards finding a continuum limit of a discrete theory involves studying coarse graining and applying renormalization methods. Note that already in flat spacetime lattice QCD [25], this is non-trivial, as one needs to study the critical behaviour of the model. In order to obtain locally covariant continuum theory, it would seem that the usual global scale transformations might be not appropriate. Some early ideas [26–28] in Spin Foam models have instead focused on defining

coarse graining via local scale transformations. A notion of refinement scale can be provided by embedding finer triangulations into coarser ones, while requiring so-called *cylindrical consistency* [3, 29–32]. Not much work has been done in this direction however, as the dynamics of Spin Foam models have not been understood beyond triangulations built out of more than few basic building blocks [4, 5]. Recently, a more global approach with the use of Tensor Network Renormalization scheme [33–35] has been used to numerically study dimensionally reduced analogue Spin Foam models - so-called spin nets [36–41], but the ideas have yet to be applied to full 4d models. Another approach under investigation is renormalization of Group Field Theories (GFT) [42–52], which generate Spin Foam amplitudes. However, the renormalizable GFTs studied so far have not been of relevance to 4d gravity. It thus still seems crucial to understand what are the dynamics of Spin Foams for configurations that can be iteratively coarse grained.

The most basic local coarse graining move on a simplicial decomposition of a manifold is a specific type of so-called Pachner moves [53]. Pachner moves are local changes of triangulation that allow to go from some triangulation of a manifold to any other triangulation in a finite number of steps. In 4 dimensions there are three different Pachner moves: The 3–3 move, 4–2 move and 5–1 move (and their inverses). An $n-(2+d-n)$ Pachner move changes a triangulation composed out of n d -simplices to one with $(2+d-n)$ d -simplices. Only the $n-1$ Pachner moves are pure coarse graining moves. The action of classical 4d Regge Calculus is known to be invariant under 5–1 and the 4–2 moves [54], but it has been a long standing open problem to make any statement about invariance under these moves for non-topological Spin Foam models. Only the naive degree of divergence of the 5–1 move has been estimated for the EPRL model [55]. This question is not even obvious in linearized gravity, as the partition function of the quantum linearized Regge Calculus has recently been found to be not invariant, as it picks up a nonlocal measure factor [56].

In this paper, we calculate the 4-dimensional Pachner moves for the first time in a Spin Foam model with simplicity constraints describing 4d Riemannian Quantum Gravity. We find that the model considered is not invariant under the 5–1 Pachner move, as the configuration of five 4-simplices reduces to a single 4-simplex with an insertion of a nonlocal operator inside. Similar behaviour occurs also for the 4–2 move. We conjecture that this is also the case for the other Spin Foam models of 4d gravity studied in the literature and discuss the possible meaning of this operator and the necessity for truncation in defining coarse graining. We then find a natural truncation scheme that allows us to make both the 4–2 and 5–1 moves invariant up to a weight depending on the boundary data. The 3–3 move is not invariant, unless very special symmetric boundary data are considered, as expected for a model of 4D Quantum Gravity.

The plan of the paper is as follows: in section II we review the construction of discretized BF theory and quantize it. We then present the diagrammatics and discuss their geometrical meaning. Next, we go on to reviewing the holomorphic representation, which simplifies the construction of $SU(2)$ invariants. This allows us to write the partition function of BF theory in the holomorphic representation. We then review the holomorphic simplicity constraints. We show that these can be imposed in two different ways. The usual way is to impose them on the boundary spin network function, resulting in the Dupuis-Livine model [12, 22], which is very similar to the EPRL-FK model. The alternative way is to impose the constraints onto a $Spin(4)$ projector. Surprisingly, the two models have the same semi-classical limit for one 4-simplex [57]. In section III we review the calculation of Pachner moves in the Ponzano-Regge model for 3d Quantum Gravity. We start with defining the notion of Pachner moves. We then discuss the gauge fixing procedure for the internal rotational $SU(2)$ symmetry. Next, we derive a crucial identity (which we refer to as the loop identity) that allows for the calculation of Pachner moves. We finish the section with calculating the 3–2 and 4–1 Pachner moves and discussing the fate of diffeomorphism symmetry. In section IV we calculate the Pachner moves in the 4d Spin Foam model constructed from the constrained projectors. We obtain the loop identity for the constrained model and find that it exhibits extra

mixing of strands in graphs, compared to the topological case. We then apply the loop identity to the 3–3, 4–2 and the 5–1 moves, and find them to be not invariant. In section V we discuss the necessity for coarse graining and show that there is a natural truncation scheme, which makes the 4–2 and 5–1 moves invariant up to a factor, while keeping the 3–3 move not invariant. We then go on to calculate and analyze the degrees of divergence of the 4–2 and 5–1 moves, and find that for a range of parameters, the latter can be divergent, while the former can be convergent. We conclude by discussing the implications of these results and the connection to recovering diffeomorphism invariance in the continuum limit of Spin Foam models.

II. HOLOMORPHIC SPIN FOAM MODELS

In this section, we will start from reviewing the discretized path integral formalism of BF theory and introducing cable diagrams notation. We will then review the holomorphic representation and the simplicity constraints. After giving a brief review of the holomorphic Spin Foam model, which was proposed in [12, 22], we will introduce an alternative model through a different imposition of these constraints. The section will end with introducing the homogeneity map, the key tool which makes the computation in this paper possible.

A. BF theory and Cable Diagrams

Spin Foam models originated from the insight that classical gravity can be described as a topological field theory (BF theory) with a simplicity constraint. As BF theory only has topological degrees of freedom, it can be easily quantized. Spin Foam models are then a path integral quantization for BF theory, with simplicity constraints imposed at the quantum level. In this section, we introduce the discretized path integral formalism of BF theory, and also give an intuitive graphic notation.

Let Δ be a simplicial complex homeomorphic to a d -dimensional manifold \mathcal{M} and let Δ^* be its dual 2-complex. The partition function of $SU(2)$ BF theory is defined in terms of the edges e and faces f of Δ^* by

$$\mathcal{Z}_{BF}(\mathcal{M}) = \int \prod_{e \in \Delta^*} dg_e \prod_{f \in \Delta^*} \delta(g_{e_1} \dots g_{e_n}). \quad (1)$$

The δ functions for each face can be expanded in representations j_f using the Peter-Weyl theorem as $\delta(g_{e_1} \dots g_{e_n}) = \sum_{j_f} (2j_f + 1) \text{tr}_{j_f}(g_1 \dots g_{e_n})$, where the trace is over the representation j_f . Inserting the resolution of identity on the representation space $V^{j_{f_1}} \otimes \dots \otimes V^{j_{f_d}}$ between each group element in the trace, we can write where $P^{j_{f_1}, \dots, j_{f_d}}$ is the projector onto the $SU(2)$ invariant subspace of $V^{j_{f_1}} \otimes \dots \otimes V^{j_{f_d}}$ given by group averaging the tensor product of irreducible representations $\rho^j : V^j \rightarrow V^j$

$$P^{j_{f_1}, \dots, j_{f_d}} = \int dg_e \rho^{j_{f_1}}(g_e) \otimes \dots \otimes \rho^{j_{f_d}}(g_e), \quad (2)$$

where the basis labels of the representations ρ^{j_f} have been suppressed. The projector is the unique map $P^{j_1, \dots, j_d} : \rho^{j_1} \otimes \dots \otimes \rho^{j_d} \rightarrow \text{Inv}_{SU(2)}[\rho^{j_1} \otimes \dots \otimes \rho^{j_d}]$, and is often called the Haar projector. For more details, see for example [2].

Cable diagrams are an intuitive and useful graphic notation, for the computations of Spin Foam partition functions (a good review of these techniques is given in [27]). Here it is used to represent the structure of partition function on the dual 2-complex Δ^* . Cable diagrams are

basically composed by strands passing through boxes: a strand denotes a representation of a symmetry group living on the edge e of Δ^* , and a box denotes the group averaging of a set of representations in the projector.

$$\rho^j = \text{---} j \text{---} \quad \text{and} \quad P^{j_1, \dots, j_d} = \begin{array}{c} j_1 \\ j_2 \\ j_3 \\ j_4 \end{array} \boxed{} \begin{array}{c} j_1 \\ j_2 \\ j_3 \\ j_4 \end{array} \quad (d = 4) \quad (3)$$

Strands form closed loops, which correspond to the faces in the dual 2-complex Δ^* . Fig.1 and Fig.2 give an example in 3 dimensions: a 3-simplex, its dual 2-complex and the corresponding cable diagram.

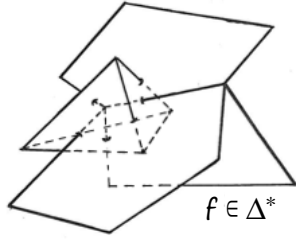


FIG. 1: A tetrahedron and its dual 2-complex

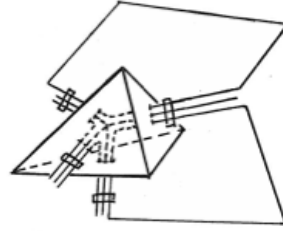


FIG. 2: A tetrahedron and its cable diagram

The projector P^{j_1, \dots, j_d} can be expressed as a sum over a basis of invariant tensors called intertwiners, as is usually done in Spin Foam models:

$$P^{j_1, \dots, j_d} = \sum_{\iota} \|j_i, \iota\rangle \langle j_i, \iota| = \sum_{\iota} \begin{array}{c} j_1 \\ j_2 \\ j_3 \\ j_4 \end{array} \rightarrow \iota \leftarrow \begin{array}{c} j_1 \\ j_2 \\ j_3 \\ j_4 \end{array} \quad (4)$$

where ι labels a basis of normalized intertwiners. We see that the projector factorizes on the edges, while the intertwiners contract at the vertices of Δ^* expressing the partition function in terms of so called vertex amplitudes. For example, if \mathcal{M} is 4 dimensional, the BF partition function can be written as

$$\mathcal{Z}_{BF}(\mathcal{M}) = \sum_{j_f} \prod_{f \in \Delta^*} (2j_f + 1) \sum_{\iota_e} \prod_{v \in \Delta^*} \begin{array}{c} \iota_{e_1} \\ \iota_{e_5} \quad \iota_{e_2} \\ \iota_{e_4} \quad \iota_{e_3} \end{array} \quad (5)$$

This is perhaps the most familiar form of BF theory. In 3d the vertex amplitudes of the Ponzano-Regge model are $6j$ symbols with no intertwiner labels since rank three intertwiners are one dimensional. In 4d the vertex amplitudes of the Oorguri model are $15j$ symbols labelled by 10 spins and 5 intertwiner labels, which are also spins. In this work, we will be most interested in the coherent state representation which can be defined in any dimension. The Livine-Speziale coherent intertwiners form an over complete basis and are labelled by a set of d spinors $\{z_i\}_{i=1}^d$. The vertex amplitude therefore depends on $d(d+1)$ spinors.

B. The Holomorphic Representation and Diagrammatics

We choose to use a spinor representation of $SU(2)$ in the Bargmann-Fock space $L_{hol}^2(\mathbb{C}^2, d\mu)$ of holomorphic polynomials of a spinor [19, 58, 59]. One of the features of this representation that will facilitate our calculations is that the Hermitian inner product is Gaussian:

$$\langle f|g\rangle = \int_{\mathbb{C}^2} \overline{f(z)} g(z) d\mu(z), \quad (6)$$

where $d\mu(z) = \pi^{-2} e^{-\langle z|z\rangle} d^4z$ and d^4z is the Lebesgue measure on \mathbb{C}^2 .

Given $z \in \mathbb{C}^2$ we denote its conjugate by \bar{z} . We use a bra-ket notation for z and square brackets \bar{z} as in

$$|z\rangle = \begin{pmatrix} z_0 \\ z_1 \end{pmatrix}, \quad [z] = \begin{pmatrix} -\bar{z}_1 \\ \bar{z}_0 \end{pmatrix}. \quad (7)$$

That is $|\bar{z}\rangle = [z]$. Notice that while $\langle z|$ is anti-holomorphic, $[z]$ is holomorphic and orthogonal to $|z\rangle$, i.e. $[z]|z\rangle = 0$. This non-standard notation for spinors will turn out to be useful, as we will always work with contractions of spinors, without the need for writing out the indices. Our notation is related to the usual one as follows: $z_A = |z\rangle_A$, $\bar{z}_{A'} = \langle z|_{A'}$, and the spinor invariants are $[z|w] = z_{A'} w_A \epsilon^{A'A}$ and $\langle z|w\rangle = \bar{z}_{A'} w_A \delta^{A'A}$. The bracket $[z|w]$ associated with the ϵ tensor is skew-symmetric, holomorphic and $SL(2, \mathbb{C})$ invariant. The bracket $\langle z|w\rangle$ associated with the identity tensor is hermitian, and only $SU(2)$ invariant.

Let us now study the identity on the Bargmann-Fock space $L_{hol}^2(\mathbb{C}^2, d\mu)$. The delta distribution on this space is given by $\delta_w(z) = e^{\langle z|w\rangle}$, since for any holomorphic function $\int d\mu(z) f(z) e^{\langle z|w\rangle} = f(w)$. Let us use a line to represent the delta graphically by

$$e^{\langle z|w\rangle} = \langle z| \text{ ————— } |w\rangle \quad \text{and} \quad \frac{\langle z|w\rangle^{2j}}{(2j)!} = \langle z| \text{ ————— }^j |w\rangle. \quad (8)$$

Therefore the Gaussian integral $\int d\mu(w) e^{\langle z|w\rangle + \langle w|z'\rangle} = e^{\langle z|z'\rangle}$ implies the contraction

$$\int d\mu(w) \langle z| \text{ ————— }^j |w\rangle \langle w| \text{ ————— }^{j'} |z'\rangle = \delta_{j,j'} \langle z| \text{ ————— }^j |z'\rangle. \quad (9)$$

For a function of four spinors (with obvious generalization to n spinors) we can thus define the *trivial projector*, which we will denote as

$$\mathbb{1}(z_i; w_i) = e^{\sum_{i=1}^4 \langle z_i|w_i\rangle} = \begin{array}{c} [z_1| \text{ ————— } |w_1\rangle \\ [z_2| \text{ ————— } |w_2\rangle \\ [z_3| \text{ ————— } |w_3\rangle \\ [z_4| \text{ ————— } |w_4\rangle \end{array}. \quad (10)$$

Next, we will study how $SU(2)$ acts on the elements of the Bargmann-Fock space. For a generic holomorphic function $f \in L_{hol}^2(\mathbb{C}^2, d\mu)$, the group action is given by

$$g \cdot f(z) = f(g^{-1}z). \quad (11)$$

The group $SU(2)$ acts irreducibly on the subspaces of holomorphic polynomials homogeneous of degree $2j$. Holomorphic polynomials with different degrees of homogeneity are orthogonal with each other. Indeed, $L_{hol}^2(\mathbb{C}^2, d\mu) = \bigoplus_{j \in \mathbb{N}/2} V^j$ and an orthonormal basis of V^j is given by

$$e_m^j(z) \equiv \frac{z_0^{j+m} z_1^{j-m}}{\sqrt{(j+m)!(j-m)!}} \quad (12)$$

and it is of dimension $2j + 1$.

In the study of gauge-invariant Spin Foam models, we will be interested in the $SU(2)$ invariant functions on n spinors

$$f(gz_1, gz_2, \dots, gz_n) = f(z_1, z_2, \dots, z_n), \quad \forall g \in SU(2). \quad (13)$$

We will denote the invariant elements of $L^2(\mathbb{C}^2, d\mu)^{\otimes n}$ to be in \mathcal{H}_n , which is the Hilbert space of n -valent intertwiners:

$$\mathcal{H}_n = \bigoplus_{j_i} \mathcal{H}_{j_1, \dots, j_n} \equiv \bigoplus_{j_i} \text{Inv}_{SU(2)} [V^{j_1} \otimes \dots \otimes V^{j_n}]. \quad (14)$$

One way to construct an element of \mathcal{H}_n is to average a function of n spinors over the group using the Haar measure. In this way we can construct a projector $P : L^2(\mathbb{C}^2, d\mu)^{\otimes n} \rightarrow \mathcal{H}_n$ which is called the Haar projector as

$$P(f)(w_i) = \int \prod_i d\mu(z_i) P(z_i; w_i) f(z_1, z_2, \dots, z_n) = \int_{SU(2)} dg f(gw_1, gw_2, \dots, gw_n) \quad (15)$$

where the kernel is given by¹

$$P(z_i; w_i) = \int_{SU(2)} dg e^{\sum_i [z_i | g | w_i]} = \begin{array}{c} [z_1 | \\ [z_2 | \\ [z_3 | \\ [z_4 | \end{array} \begin{array}{c} \text{---} \boxed{} \text{---} \\ \text{---} \boxed{} \text{---} \\ \text{---} \boxed{} \text{---} \\ \text{---} \boxed{} \text{---} \end{array} \begin{array}{c} |w_1\rangle \\ |w_2\rangle \\ |w_3\rangle \\ |w_4\rangle \end{array}, \quad (16)$$

where we use a box to represent group averaging with respect to the Haar measure over $SU(2)$. Hence the projector onto the invariant subspace is simply the group average of $\mathbb{1}(z_i; w_i)$. From the above, we see that a contraction of two spinors on the same strand but belonging to two different projectors is obtained by setting $z_i^1 = \check{w}_i^2$. This implies that the kernel of the projector satisfies the projection property

$$\int \prod_i d\mu(w_i) P(z_i; w_i) P(\check{w}_i; z'_i) = P(z_i; z'_i). \quad (17)$$

We will also refer from now on to the kernel $P(z_i; w_i)$ as a projector for convenience. As shown in [17, 24], we can perform the integration over g in Eq. (16) explicitly, which gives a power series in the holomorphic spinor invariants:

$$P(z_i; w_i) = \sum_{[k]} \frac{1}{(J+1)!} \prod_{i < j} \frac{([z_i | z_j][w_i | w_j])^{k_{ij}}}{k_{ij}!}, \quad (18)$$

where the sum is over a set of $n(n-1)/2$ non-negative integers $[k] \equiv (k_{ij})_{i \neq j=1, \dots, n}$ with $1 \leq i < j \leq n$ and $k_{ij} = k_{ji}$. A short proof of this statement is given in the Appendix C for the reader's convenience. Thus a basis of n -valent intertwiners is given by

$$(z_i | k_{ij}) \equiv \prod_{i < j} \frac{[z_i | z_j]^{k_{ij}}}{k_{ij}!}. \quad (19)$$

¹ For a review of Gaussian integration techniques see Appendix A.

The non-negative integers $(k_{ij})_{i \neq j=1, \dots, n}$ are satisfying the n homogeneity conditions

$$\sum_{j \neq i} k_{ij} = 2j_i. \quad (20)$$

The sum of spins at the vertex is defined by $J = \sum_i j_i = \sum_{i < j} k_{ij}$ and is required to be a positive integer. We also see from Eq. (18) that the identity on \mathcal{H}_{j_i} is resolved as follows

$$\mathbb{1}_{\mathcal{H}_{j_i}} = \sum_{[k] \in K_j} \frac{|k_{ij}\rangle \langle k_{ij}|}{\|k_{ij}\|^2}, \quad \|k_{ij}\|^2 = \frac{(J+1)!}{\prod_{i < j} k_{ij}!}. \quad (21)$$

with the set K_j defined by integers k_{ij} satisfying Eq.(20). For more details on these intertwiners and the coherent states defined by them, see [64] where this basis was introduced for the first time.

Before we go on to the discussion of simplicity constraints, let us notice that using a multinomial expansion Eq.(18) can be written in terms of total spin:

$$P(z_i; w_i) = \sum_{J=0}^{\infty} \frac{\left(\sum_{i < j} [z_i | z_j] \langle w_i | w_j \rangle \right)^J}{J!(J+1)!}, \quad (22)$$

which will turn out to be a quite useful expression for the projector for computation purposes. Note that this is an expansion in $U(N)$ coherent intertwiners of total area J .

C. Holomorphic Simplicity Constraints

Holomorphic simplicity constraints for spinorial Spin Foam models were first introduced in [12] for Riemannian gravity. Here we give a short summary, but refer the reader to the original paper for their full derivation.

For the Riemannian 4d Spin Foam models, we use the gauge group $\text{Spin}(4) = \text{SU}(2)_L \times \text{SU}(2)_R$, which is the double cover of $\text{SO}(4)$. The holomorphic simplicity constraints are isomorphisms between the two representation spaces of $\text{SU}(2)$: for any two edges i, j that are a part of the same vertex a , they are defined by

$$[z_{iL}^a | z_{jL}^a] = \rho^2 [z_{iR}^a | z_{jR}^a], \quad (23)$$

where ρ is a function of the Immirzi parameter γ given by

$$\rho^2 = \begin{cases} (1 - \gamma)/(1 + \gamma), & |\gamma| < 1 \\ (\gamma - 1)/(1 + \gamma), & |\gamma| > 1 \end{cases} \quad (24)$$

The holomorphic simplicity constraints Eq.(23) essentially tell us that there exists a unique group element $g_a \in \text{SL}(2, \mathbb{C})$ for each vertex a , such that

$$\forall i, \quad g_a |z_{iL}^a\rangle = \rho |z_{iR}^a\rangle. \quad (25)$$

A general element of $\text{SL}(2, \mathbb{C})$ can be decomposed into the product of an hermitian matrix times an element of $\text{SU}(2)$, so that $g_a = h_a u_a$ with $h_a^\dagger = h_a$. It is only when $h_a = \mathbb{1}$ that the holomorphic simplicity constraints imply the usual geometrical simplicity constraints. In the FK formulation of the spin foam model which is only partially holomorphic this is implied since the norm of the spinors is fixed. The fully holomorphic formulation of DL therefore relaxes at the quantum level the simplicity constraints. Fortunately, one can check following [64] that in the semi-classical limit

of Holomorphic amplitudes the Gauss constraints due to the gauge invariance of the amplitude can be realized in the form

$$\sum_i |z_{iL}^a\rangle\langle z_{iL}^a| = A_L \mathbb{1}, \quad \sum_i |z_{iR}^a\rangle\langle z_{iR}^a| = A_R \mathbb{1}. \quad (26)$$

This imposes that in the classical limit $h_a = 1$ and the geometrical simplicity constraints $u_a |z_{iL}^a\rangle = \rho |z_{iR}^a\rangle$ with $u_a \in \text{SU}(2)$ are satisfied.

Let us recall the geometrical meaning of these: Each spinor defines a three vector $\vec{V}(z) \in \mathbf{R}^3$ through the equation

$$|z\rangle\langle z| = \frac{1}{2} \left(\mathbb{1}\langle z|z\rangle + \vec{V}(z) \cdot \vec{\sigma} \right), \quad |z][z| = \frac{1}{2} \left(\mathbb{1}[z|z] - \vec{V}(z) \cdot \vec{\sigma} \right) \quad (27)$$

where $\vec{\sigma}$ is the vector made by Pauli matrices. Thus around a vertex in a spin-network, each link dual to a triangle in the simplicial manifold, is associated with two 3-vectors $\vec{V}_L(z)$ and $\vec{V}_R(z)$ given by the left and right spinors. Classically, they correspond to the selfdual b_+ and anti-selfdual b_- components of the B field respectively :

$$V_L^i(z) = b_+^i := B^{0i} + \frac{1}{2}\epsilon_{kl}^i B^{kl}, \quad V_R^i(z) = b_-^i := -B^{0i} + \frac{1}{2}\epsilon_{kl}^i B^{kl}. \quad (28)$$

Note here that the time norm is chosen to be $N_I = (1, 0, 0, 0)^T$. For the Hodge dual of the B field, we find $(*b)_+ = b_+ = \vec{V}_L(z)$, and $(*b)_- = -b_- = -\vec{V}_R(z)$.

For the vectors $\vec{V}_L(z)$ and $\vec{V}_R(z)$ defined by the spinors of the two copies of $\text{SU}(2)$ this means that the holomorphic simplicity constraints imply

$$g_a \triangleright \vec{V}_L(z_i^a) = \rho^2 \vec{V}_R(z_i^a), \quad \forall i \in a \quad (29)$$

which leads to the constraint that the norm of the selfdual and anti-selfdual components of the bivector $(g_a, \mathbb{1}) \triangleright (B + \gamma * B)$ have to be equal to each other:

$$|(1 + \gamma)g_a \triangleright b_+| = |(1 - \gamma) \triangleright b_-|. \quad (30)$$

Thus B and $*B$ are simple bivectors, and for the spin network vertex a , there exists a common time norm to all the bivectors:

$$\mathcal{N}_a = (g_a, \mathbb{1})^{-1} \triangleright (1, 0, 0, 0). \quad (31)$$

The existence of this shared time norm implies the linear simplicity constraints introduced by the EPRL and FK models [8–11].

It is interesting to note that g_a can be expressed purely in terms of spinors as

$$g_a = \frac{|z_{iR}^a\rangle\langle z_{iL}^a| + |z_{iR}^a][z_{iL}^a|}{\sqrt{\langle z_{iL}^a|z_{iL}^a\rangle\langle z_{iR}^a|z_{iR}^a\rangle}}, \quad \forall i \in a. \quad (32)$$

It is easy to check that this satisfies Eq. (25). Note here that g_a is a unique group element for all strands belonging to the same vertex.

D. Imposing constraints

We will now impose the holomorphic simplicity constraints on the $\text{Spin}(4)$ BF theory in order to obtain a model of 4d Riemannian Quantum Gravity. There are two natural ways of imposing these

constraints - either on the boundary spin network defined by contraction of coherent states [12], or on the whole projector (16). We will first summarize the usual approach, which we will refer to as the DL prescription. Then we will introduce an alternative model in which the constraint is imposed on the whole projector. It is very surprising that the alternative model actually has the same asymptotic behavior [57] as the DL prescription and EPRL/FK model (with $|\gamma| < 1$) [60–62], i.e. the amplitude is weighted by a cosine of the Regge [63] action. It leads however to a much simpler calculation when we evaluate the Pachner moves than the DL case. Even though there is no technical obstacle to use the DL prescription, we will study it in a subsequent article, and focus on the constrained projector model in this paper.

1. DL prescription

In [12, 22] Dupuis and Livine introduced a Spin Foam model similar to the EPRL/FK models, but written in terms of spinorial coherent states with the holomorphic simplicity constraints. Since BF amplitudes can be seen as evaluations of spin network functions, the simplicity constraints in this model are imposed in the usual way – on the boundary spin network given by the amplitude. The amplitude for a single 4-simplex σ is given by a product of contraction of coherent states for left and right sectors, with the simplicity constraints imposed on the boundary spinors as follows

$$\mathcal{A}_\sigma(\{z_\Delta^\tau\}) = \int [dg_\tau^L]^5 [dg_\tau^R]^5 e^{\sum_{\Delta \in \sigma} \rho^2 [z_\Delta^{s(\Delta)} | g_{s(\Delta)}^L]^{-1} g_{t(\Delta)}^L | z_\Delta^{t(\Delta)} \rangle + [z_\Delta^{s(\Delta)} | g_{s(\Delta)}^R]^{-1} g_{t(\Delta)}^R | z_\Delta^{t(\Delta)} \rangle} \quad (33)$$

where Δ label different triangles/strands and $\tau, s(\Delta), t(\Delta)$ label tetrahedra/projectors. Graphically this is presented in Fig. 3. This amplitude corresponds to two copies of 20j symbols from BF theory

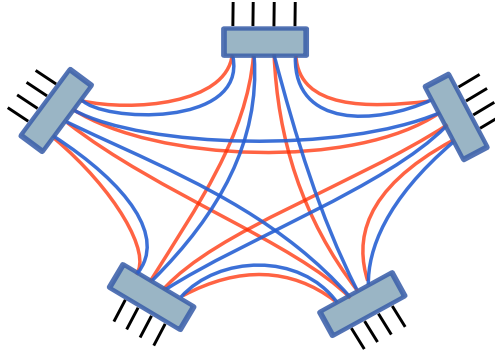


FIG. 3: Graph for the 4-simplex amplitude in the DL model. The contractions inside correspond to two copies of BF 20j symbols, constrained on the boundary.

constrained by $[z_L^{s(\Delta)} | z_L^{t(\Delta)} \rangle = \rho^2 [z_R^{s(\Delta)} | z_R^{t(\Delta)} \rangle$ on the boundary.

2. Constrained projector

Since spin foam amplitudes for BF theory are constructed by gluing together projectors (22) into graphs corresponding to 4d quantum geometries, we find it natural to instead impose the constraints on the arguments of the projectors themselves. Let us consider the Spin(4) projector obtained by taking a product of two SU(2) projectors

$$P(z_i; w_i) P(z'_i; w'_i) = \sum_J \frac{\left(\sum_{i < j} [z_i | z_j] [w_i | w_j] \right)^J}{J! (J+1)!} \sum_{J'} \frac{\left(\sum_{i < j} [z'_i | z'_j] [w'_i | w'_j] \right)^{J'}}{J'! (J'+1)!}, \quad (34)$$

where we use a prime to distinguish the left and right SU(2) sectors. We will now impose the holomorphic simplicity constraints on both incoming and outgoing strands in the Spin(4) projector

$$[z'_i|z'_j\rangle = \rho^2[z_i|z_j\rangle \quad [w'_i|w'_j\rangle = \rho^2[w_i|w_j\rangle.$$

This will make the two products of spinors in the two projectors proportional to each other, with the proportionality constant being ρ^4 . Note that the imposition of simplicity constraints on all of the spinors also forces the measure of integration on \mathbb{C}^2 to change to

$$d\mu_\rho(z) := \frac{(1 + \rho^2)^2}{\pi^2} e^{-(1+\rho^2)\langle z|z\rangle} d^2z. \quad (35)$$

The factor of $(1 + \rho^2)^2$ is added for normalization. It insures that

$$\int d\mu_\rho(z) = 1. \quad (36)$$

Moreover this choice of normalization is confirmed by the study of asymptotics of both this and the DL model [57]. It is exactly this choice that insures that both models have the same semi-classical limit. We are now ready to define a new *constrained propagator* P_ρ by applying the simplicity constraints on the Spin(4) projector

$$P_\rho(z_i; w_i) \equiv P(z_i; w_i)P(\rho z_i; \rho w_i) = \sum_J \sum_{J'} \frac{\rho^{4J'}}{J!(J+1)!J'!(J'+1)!} \left(\sum_{i < j} [z_i|z_j\rangle [w_i|w_j\rangle \right)^{J+J'}. \quad (37)$$

The two sums over integers J and J' are independent, so we can simplify this expression for the constrained propagator into a single sum by letting $J + J' \rightarrow J$. This allows us to arrive at a more compact form of the constrained propagator, given by

$$P_\rho(z_i; w_i) = \sum_J F_\rho(J) \frac{\left(\sum_{i < j} [z_i|z_j\rangle [w_i|w_j\rangle \right)^J}{J!(J+1)!}, \quad (38)$$

where we have recognized that the numerical factor in front of the spinors is actually the power series expansion of the hypergeometric function

$$F_\rho(J) := {}_2F_1(-J-1, -J; 2; \rho^4) = \sum_{J'=0}^J \frac{J!(J+1)!\rho^{4J'}}{(J-J')!(J-J'+1)!J'!(J'+1)!}. \quad (39)$$

Notice that the constrained Spin(4) propagator is just an SU(2) projector with non-trivial weights (greater than 1) for each term that depend on the Barbero-Immirzi parameter. In general, this hypergeometric function is a complicated function of ρ , but let us look at two interesting limiting cases. For $\rho = 0$, which corresponds to $\gamma \rightarrow 1$, we have

$${}_2F_1(-J-1, -J; 2; 0) = 1, \quad (40)$$

so we end up with pure SU(2) BF theory. This is obvious, as $\rho = 0$ forces all the left spinors to be 0. Another limit often considered is $\rho = 1$, which in this construction surprisingly corresponds to both of the limits $\gamma \rightarrow 0$ and $\gamma \rightarrow \infty$. In this limit we get also a relatively simple expression

$${}_2F_1(-J-1, -J; 2; 1) = \frac{(2J+2)!}{(J+2)!(J+1)!}. \quad (41)$$

This limit does not have an obvious interpretation apart from its simplicity.

We can now define the partition function for the Spin Foam model made up from these constrained propagators. Since the propagators are just BF projectors with non-trivial weight, we can write the partition function on a 2-complex Δ^* as

$$\mathcal{Z}_G^{\Delta^*} = \sum_{j_f} \prod_{f \in \Delta^*} \mathcal{A}_f(j_f) \int \left\{ \prod_{all} d\mu_\rho(z) d\mu_\rho(w) \right\} \sum_{k_{ff'} \in K_j} \prod_e P_\rho^{k_{ij}}(z_i^e; w_i^e), \quad (42)$$

where $\mathcal{A}_f(j_f)$ is a face weight, the set K_j was defined previously in Eq. (20) to be the set of integers k_{ij} satisfying $\sum_{i \neq j} k_{ij} = 2j_i$ and contraction of spinors according to the 2-complex Δ^* on different edges is implied. The constrained propagator at fixed spins is given by

$$P_\rho^{k_{ij}}(z_i^e; w_i^e) := \frac{F_\rho(J_e)}{(J_e + 1)!} \prod_{i < j} \frac{([z_i^e | z_j^e][w_i^e | w_j^e])^{k_{ij}}}{k_{ij}!}. \quad (43)$$

Each constrained propagator comes with an orientation, with spinors z incoming into the box and spinors w outgoing in this paper's convention. A change of this edge orientation results in overall minus sign for the amplitude. Additionally we also put an orientation on each strand, which dictates how spinors on different propagators are contracted. An example is shown in Fig. 4. When we glue 4-simplices, we have two propagators contracted on the dual edge along which they are glued.

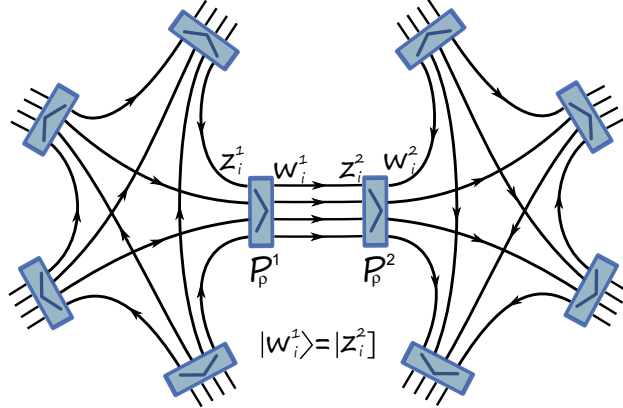


FIG. 4: Graph for the amplitude of contraction of two 4-simplices. Propagators P_ρ^1 and P_ρ^2 belong to the same edge but two different 4-simplices. The spinors belonging on the same strand but belonging to different propagators are contracted according to the strand orientation. For example, spinors $w_i^1 = z_i^2$.

It is interesting to note here that, unlike in the usual Spin Foam models, this definition in terms of propagators does not necessarily constrain the partition function to be a product of vertex amplitudes, thus allowing for more general non-geometrical structures.

E. The Homogeneity Map

In this section we will introduce a very useful tool that will allow us to make calculations of Pachner moves more tractable. Notice that the propagator P_ρ is a polynomial obtained from products of monomials $[z_i | z_j][w_i | w_j]^{k_{ij}}$ which possess a degree of homogeneity of $4k_{ij}$. These

products of monomials of different homogeneity degrees are orthogonal in the Bargmann-Fock space. The homogeneity property allows us to always separate out and track terms of given homogeneity in a power series expansion. This means that we can perform transformations term by term in the series expansion of the propagator and independently integrate each term.

Let us hence define a more general propagator G_τ that can be exponentiated

$$G_\tau(z_i; w_i) = \sum_J \tau^J \frac{\left(\sum_{i < j} [z_i | z_j] [w_i | w_j] \right)^J}{J!} = e^{\tau \sum_{i < j} [z_i | z_j] [w_i | w_j]} \quad (44)$$

and denote it graphically by

$$G_\tau(z_i; w_i) = \begin{array}{c} [z_1| \\ [z_2| \\ [z_3| \\ [z_4| \end{array} \begin{array}{c} \text{---} \\ \text{---} \\ \text{---} \\ \text{---} \end{array} \begin{array}{c} \boxed{\tau} \\ \boxed{\tau} \\ \boxed{\tau} \\ \boxed{\tau} \end{array} \begin{array}{c} \text{---} \\ \text{---} \\ \text{---} \\ \text{---} \end{array} \begin{array}{c} |w_1\rangle \\ |w_2\rangle \\ |w_3\rangle \\ |w_4\rangle \end{array}. \quad (45)$$

We can see that τ^J tracks homogeneity of the polynomial in spinors. If we transform each of these τ^J into a function of J , the integrals of the polynomials stay the same. In this way we can perform complicated calculations with G_τ and in the end we can use the following map, defined by a functional H_f mapping G_τ to the desired function f :

$$H_\rho : G_\tau \rightarrow P_\rho \quad \text{with} \quad H_\rho : \tau^J \rightarrow \frac{F_\rho(J)}{(J+1)!} \quad (\text{Simplicity Constraints}) \quad (46)$$

$$H_P : G_\tau \rightarrow P \quad \text{with} \quad H_P : \tau^J \rightarrow \frac{1}{(J+1)!} \quad (\text{BF Theory}) \quad (47)$$

in order to recover the propagators of the BF theory or the one of the gravity model with simplicity constraints imposed. Note that $P_0 = P$ so the BF model is included in our more general description. We are of course not limited to only these choices and could in principle study a much wider class of spin foam models built by non-trivial propagators.

By considering how BF projectors compose in Eq. (17), it is quite easy to find the homogeneity map for composing the propagator P_ρ n times: $P_\rho \circ \dots \circ P_\rho$. To do this, we just realize that if one reintroduces back the factor of $1/(J+1)!$ into the definition of G_τ , it then defines just the BF projector P with the spinors z rescaled to $\sqrt{\tau}z$. The homogeneity map for the composition is therefore given by²

$$\tau^J \rightarrow \frac{F_\rho(J)^n}{(J+1)!(1+\rho^2)^{2(n-1)J}} \quad \text{for} \quad G_\tau \rightarrow P_\rho^n \quad (n \text{ Propagators}). \quad (48)$$

For the purpose of calculating Pachner moves, we will need to consider contracted loops of spinors. In BF theory, such a loop should correspond to an $SU(2)$ delta function. Using the spinorial language however, we get

$$\begin{array}{c} \text{---} \\ \text{---} \\ \text{---} \\ \text{---} \end{array} \begin{array}{c} \text{---} \\ \text{---} \\ \text{---} \\ \text{---} \end{array} = \int d\mu(z) e^{\langle z | z \rangle} = \sum_j \int d\mu(z) \frac{\langle z | z \rangle^{2j}}{(2j)!} = \sum_j \chi^j(\mathbb{1}) = \sum_j (2j+1), \quad (49)$$

² Note that the factor of $(1+\rho^2)^{2J}$ in (46) comes from the fact that the measure has changed under the simplicity constraints to $d\mu_\rho(z) = (1+\rho^2)^2 \pi^{-2} e^{-(1+\rho^2)\langle z | z \rangle}$. Hence every contraction produces a factor $(1+\rho^2)^{-2j}$ where j is the representation of the line. There is one such contraction for each j where $J = \sum j$ for each τ .

whereas a delta function is $\delta_{SU(2)}(\mathbb{1}) = \sum_j (2j+1)^2$. One way of going around this is to change measure of integration for this loop to $d\tilde{\mu}(z) = (\langle z|z \rangle - 1)d\mu(z)$, as was suggested in [22]. This provides the additional factor of $(2j+1)$. An alternative way is to follow in the spirit of the homogeneity map and introduce a τ' that tracks the homogeneity in this loop. For clarity, we add a symbol for this face weight into the graph:

$$\text{Diagram of a loop with a face weight } f \text{ inside} = \int d\mu(z) e^{\tau' \langle z|z \rangle} = \sum_j \tau'^{2j} (2j+1). \quad (50)$$

The replacement of $\tau'^{2j} \rightarrow (2j+1)$ now defines a homogeneity map for a BF loop. Of course, we now do not have to restrict ourselves to this simple face weight and can choose an arbitrary function of spin.

The homogeneity map we have developed in this section will be very useful in computing the 4-dimensional Pachner moves. In later sections we will define additional homogeneity maps as we go on, to simplify the calculations.

III. PACHNER MOVES IN 3D QUANTUM GRAVITY

In this section we review the notion of Pachner moves and their calculation in 3d $SU(2)$ BF theory, to set up the stage for comparison to the 4-dimensional models. A crucial tool that allows the calculation is a so called *loop identity*, which we will derive in the holomorphic representation.

A. Definition of Pachner Moves

To show that a theory defined on a triangulated manifold is topologically invariant, we need a way to relate different triangulations. This is provided by the Pachner moves, which are local replacements of a set of connected simplices by another set of connected simplices.

Theorem III.1. *Any simplicial piecewise linear manifold \mathcal{M} can be transformed into any other simplicial piecewise linear manifold \mathcal{M}' homeomorphic to \mathcal{M} by a finite sequence of Pachner moves.*

For proof, see [53].

Pachner moves are constructed by adding (or removing) vertices, edges, triangles etc. to (from) the existing triangulation. They can be also obtained in d dimensions by gluing a $(d+1)$ -simplex onto the d -dimensional triangulation. There are several Pachner moves in each dimension and they correspond to changing a configuration of n basic building blocks (d -simplices) into a configuration of m building blocks - we call them n - m Pachner moves. In two dimensions we hence have the moves 2-2, 1-3 moves and their reverse. The 2-2 move corresponds to changing the edge along which two triangles are glued, while the 1-3 move corresponds to adding a vertex inside a triangle and connecting it to the other vertices by three edges, arriving in a configuration with three triangles. Fig. 5 shows the inverse. In three dimensions we have 3-2, 4-1 moves and their reverse, see Fig. 6. The 3-2 move corresponds to removing an edge, along which three tetrahedra were glued and changing it into a configuration of two tetrahedra. The 4-1 move is combining four tetrahedra into one tetrahedron through removing a common vertex.

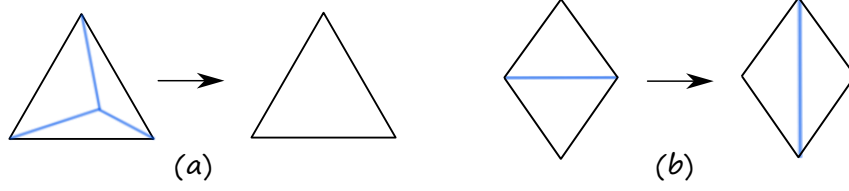


FIG. 5: Two dimensional Pachner moves: a) 3–1 move, in which three triangles are merged into one by removing a vertex inside; b) 2–2 move, in which two triangles exchange the edge, along which they are glued.

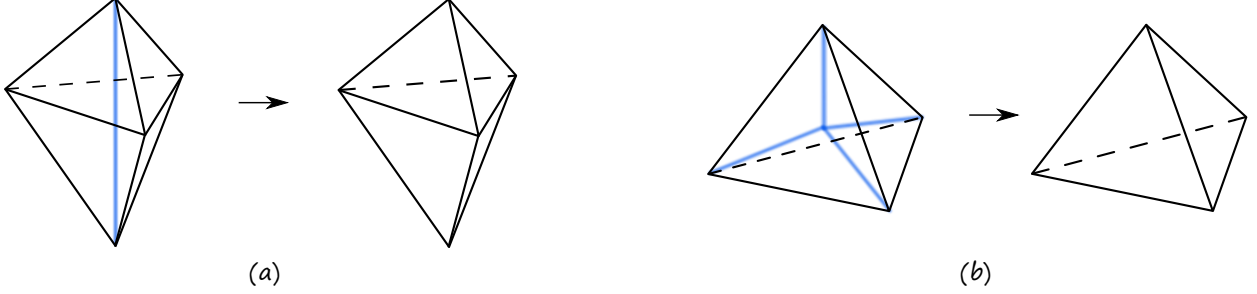


FIG. 6: Three dimensional Pachner moves: a) 3–2 move, in which three tetrahedra are changed into two tetrahedra by removing a common edge; b) 4–1 move, in which four tetrahedra are combined into one by removing a common vertex.

B. Fixing the gauge

3-dimensional gravity, as described by BF theory, has two important gauge symmetries – internal rotational “Lorentz” $SU(2)$ gauge symmetry and the *translational* symmetry [65] following from the Bianchi identity $d_\omega F = 0$. The action can be explicitly written as

$$S[e, \omega] = \int_{\mathcal{M}} \text{Tr} [e \wedge (d\omega + \omega \wedge \omega)]. \quad (51)$$

The local Lorentz gauge transformations δ^L and the translational symmetry transformations δ^T are given by

$$\begin{aligned} \delta_X^L \omega &= d_\omega X, & \delta_X^L e &= [e, X] \\ \delta_X^T \omega &= 0, & \delta_X^T e &= d_\omega X, \end{aligned} \quad (52)$$

where the parameter of transformations is an $\mathfrak{su}(2)$ Lie algebra element X . There is also obviously the diffeomorphism symmetry generated by a vector field ξ_μ , but one can show [65] that on-shell we have

$$\delta_\xi^D = \delta_{\iota_\xi \omega}^L + \delta_{\iota_\xi e}^T, \quad (53)$$

i.e. the three symmetries are related.

Let us now understand how to fix the “Lorentz” gauge on a spin network. Since the volume of the group $SU(2)$ is finite, the gauge fixing amounts to only a change of variables along a maximal tree. We follow [66] in defining the gauge fixing procedure. Consider a graph Γ with E edges and V vertices. Each edge is oriented so that it starts at a source vertex $s(e)$ and ends at target $t(e)$. Consider now a spin network function such that

$$\psi^\Gamma(g_{e_1}, \dots, g_{e_E}) = \psi^\Gamma(h_{s(e_1)}^{-1} g_{e_1} h_{t(e_1)}, \dots, h_{s(e_E)}^{-1} g_{e_E} h_{t(e_E)}). \quad (54)$$

Now choose a maximal tree T in Γ , i.e. a collection of $V - 1$ edges which passes through every vertex, without forming loops. Choose a vertex A to be the root³ of the tree T and label g_{vA}^T the product of group elements g_{e_i} along T that connect vertex v and A . Next we will use Eq. (54) with $h_v = g_{vA}^T$, so that $\psi^\Gamma = \psi^\Gamma(G_1^T, \dots, G_E^T)$ with $G_e^T = g_{As(e)}^T g_e g_{t(e)A}^T$.

Now, for any edge $e \in T$, there is a unique path along the tree connecting A and $s(e)$ or $t(e)$. Let us choose this to be $t(e)$, since the other case works in the same way. It follows that $g_{s(e)A}^T = g_e g_{t(e)A}^T$ and so $G_e^T = \mathbb{1}$ for $e \in T$. Hence the procedure for gauge fixing is to set all the group elements on the maximum tree to $\mathbb{1}$ and change all the other to $g_{e_i} = G_{e_i}^T$. Since $\int_{SU(2)} dg = 1$, ending up with empty integrations does not lead to any divergences. In the language of amplitudes written in terms of projectors, this corresponds to replacing the projectors $P(z_i; w_i) = \int_{SU(2)} dg e^{\sum_i [z_i | g | w_i]}$ on the maximal tree by the trivial propagators $\mathbb{1}(z_i; w_i) \equiv e^{\sum_i [z_i | w_i]}$. This procedure carries over to the 4-dimensional case trivially, since $\text{Spin}(4)$ is just a product $SU(2) \times SU(2)$.

We will postpone the discussion of the translational symmetry to until after we have calculated the 4-1 Pachner move, as we will see that it is directly related to the divergence coming from that calculation. However, in 4-dimensional Spin Foam models the relation between divergences and translational symmetry is unknown – we will discuss this in Section V.

C. The Loop Identity

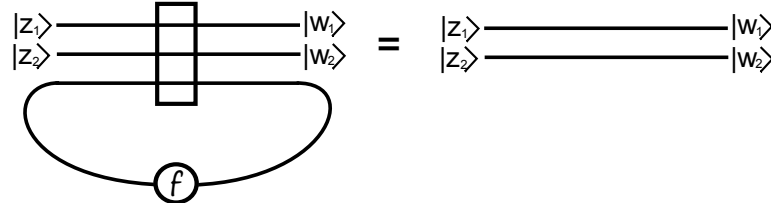
The BF theory partition function is independent of the triangulation Δ . This can be shown by demonstrating its invariance (up to an overall factor) with respect to a finite set of coarse graining moves, constructed out of Pachner moves. The Pachner moves can all be derived from one identity which we will call the loop identity. This identity follows from the coherent state representation of the $SU(2)$ delta function

$$\delta(g) = \int d\tilde{\mu}(z) e^{\langle z | g | z \rangle}, \quad (55)$$

where $d\tilde{\mu}(z) = d\mu(z)(\langle z | z \rangle - 1)$. Therefore

$$\begin{aligned} \int d\tilde{\mu}(z_n) P(z_1, \dots, z_n; w_1, \dots, w_n) &= \int dg e^{\sum_{i=1}^{n-1} [z_i | g | w_i]} \int d\tilde{\mu}(z_n) e^{[z_n | g | z_n]} \\ &= \int dg e^{\sum_{i=1}^{n-1} [z_i | g | w_i]} \delta(g) \\ &= e^{\sum_{i=1}^{n-1} [z_i | w_i]} \\ &= \mathbb{1}(z_1, \dots, z_{n-1}; w_1, \dots, w_{n-1}), \end{aligned} \quad (56)$$

which is represented graphically by



$$(57)$$

Since each closed loop of the BF partition function (5) has a factor of $2j_f + 1$ we will use the convention that two lines are contracted with $d\mu(z)$ as in (9), however, the contraction of a line

³ One can show that the gauge fixing procedure is independent of this choice.

with itself, i.e. a loop, is contracted with the measure $d\tilde{\mu}(z)$ as in (57). An alternative way would be to use the homogeneity map to keep track of this face weight.

D. Alternative method

The expression for the loop identity we have just derived, while compact, does not generalize straightforwardly to the case of 4-dimensional QG models with simplicity constraints (due to the presence of the group integrals). We will thus redo the above calculation with the projector written in terms of only spinors without group integration.

We expect that the loop identity (56) applied to the projector (22) implies that

$$\sum_{j_n} (2j_n + 1) \int d\mu(z_n) \frac{\left(\sum_{i < j} [z_i | z_j] [w_i | w_j] \right)^J}{J! (J + 1)!} = \prod_{i=1}^{n-1} \frac{[z_i | w_i]^{2j_i}}{(2j_i)!}, \quad (58)$$

where the integration is performed with $w_n = \check{z}_n$. Below we will directly show this. Let us perform the integration on the LHS explicitly by using the homogeneity map to keep track of the $1/(J + 1)!$ and the face weight $(2j_n + 1)$ and then summing over j_i . Namely, let us use the homogeneity maps $\tau^J \rightarrow 1/(J + 1)!$ and $\tau'^{2j_n} \rightarrow (2j_n + 1)$. The result is then

$$\int d\mu(z_n) \exp \left(\tau \sum_{i < j < n} [z_i | z_j] [w_i | w_j] - \tau \tau' \sum_{i < n} \langle z_n | z_i \rangle [w_i | z_n] \right) = \frac{e^{\tau \sum_{i < j < n} [z_i | z_j] [w_i | w_j]}}{\det (\mathbb{1} - \tau \tau' \sum_{i < n} |w_i\rangle [z_i|])}. \quad (59)$$

To continue, we have to be able to evaluate the determinant in the denominator. This is thankfully not too difficult, as the matrix in question is just a 2×2 matrix made up by spinors. Indeed, the following lemma comes in handy

Lemma III.2. *Let $M = \mathbb{1} - \sum_i C_i |A_i\rangle [B_i|$ then*

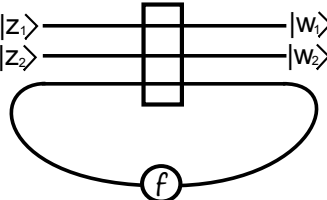
$$\det M = 1 - \sum_i C_i [B_i | A_i] + \sum_{i < j} C_i C_j [A_i | A_j] [B_i | B_j].$$

The proof is given in Appendix D.

Using this result, we can immediately find the determinant in (59). In our case, all $C_i = \tau \tau'$, hence we get that the loop identity for the homogenized projector P_τ becomes

$$\frac{e^{\sum_{1 \leq i < j < n} \tau \tau' [z_i | z_j] [w_i | w_j]}}{1 - \sum_{i \neq n} \tau \tau' [z_i | w_i] + \sum_{1 \leq i < j < n} \tau^2 \tau'^2 [z_i | z_j] [w_i | w_j]}. \quad (60)$$

Now we can expand both the numerator and the denominator in a power series and then use the homogeneity map to restore the $1/(J + 1)!$ terms and the face weight. This allows us to get the loop identity for the projector (22)



$$= \sum_{J, J'} C_{BF}(J, J') \left(\sum_{i < n} [z_i | w_i] \right)^J \left(\sum_{i < j < n} [z_i | z_j] [w_i | w_j] \right)^{J'}, \quad (61)$$

where we have defined the coefficient $C_{BF}(J, J')$ to be given by

$$C_{BF}(J, J') = \sum_K (-1)^{J'-K} \frac{(J + J' - K)!(J + 2J' - 2K + 1)}{J!(J' - K)!K!(J + 2J' - K + 1)!}. \quad (62)$$

At first glance, this is a worrisome result, as we do not only get the trivial projection (raised to power J), but also an unwanted *mixing* term (raised to power J'). Notice though, that we have an additional free sum over the variable K in the definition of the coefficient. We can actually explicitly evaluate this sum over K to find the expected result

$$C_{BF}(J, J') = \frac{\delta_{J',0}}{J!}. \quad (63)$$

Hence only the $J' = 0$ term is non-vanishing, so the mixing terms always drop out in BF theory. We thus recover the result (58) that we set out to prove. This calculation readily is generalized in the following section to the case with simplicity constraints. The major difference in this case is the lack of the cancellation of the mixing terms.

E. Invariance under Pachner moves and symmetry

We will now proceed to show the invariance of the 3-dimensional $SU(2)$ BF theory under 3-2 and 4-1 Pachner moves using the language of spinors. In the case of 4-1 move we find a divergence directly related to the translational symmetry.

1. 3-2 move

As can be seen in the Fig. 6 a), the configuration of three tetrahedra in the 3-2 move is glued along one edge. This corresponds to a loop of a single strand in the cable diagram, see Fig.7.

By choosing a maximum tree (with a root at the projector 1) in the diagram, we can gauge fix the projectors number 7 and 9. This allows us to apply the loop identity (56) to integrate out the strand number 10 by performing the group integral in projector number 8. We can identify now that the resulting cable diagram is exactly that of the two tetrahedra glued together, see Fig. 6 b). Hence it is immediate that the $SU(2)$ BF theory is invariant under the 3-2 Pachner move, as the two configurations are gauge equivalent.

2. 4-1 move

The configuration of four tetrahedra in the 4-1 move shares in total four edges, which corresponds to four loops in a cable diagram, see Fig. 8 a).

We choose a maximum tree with a root at vertex 1, which allows us to gauge fix the projectors number 5, 6 and 9. We can now apply the loop identity (56) to the projector 10 to remove the blue loop. Similarly we can apply the loop identities to projectors 7 and 8 to remove the yellow and green loops respectively. This leaves us with the last loop and no projectors left inside the graph, as in Fig. 8 b). This final loop corresponds to the following integral

$$\begin{aligned} \int d\tilde{\mu}(z) e^{\langle z|z \rangle} &= \sum_j \int d\tilde{\mu}(z) \frac{\langle z|z \rangle^{2j}}{(2j)!} = \sum_j (2j+1) \int d\mu(z) \frac{\langle z|z \rangle^{2j}}{(2j)!} \\ &= \sum_j (2j+1) \chi^j(\mathbb{1}) = \delta_{SU(2)}(\mathbb{1}). \end{aligned} \quad (64)$$

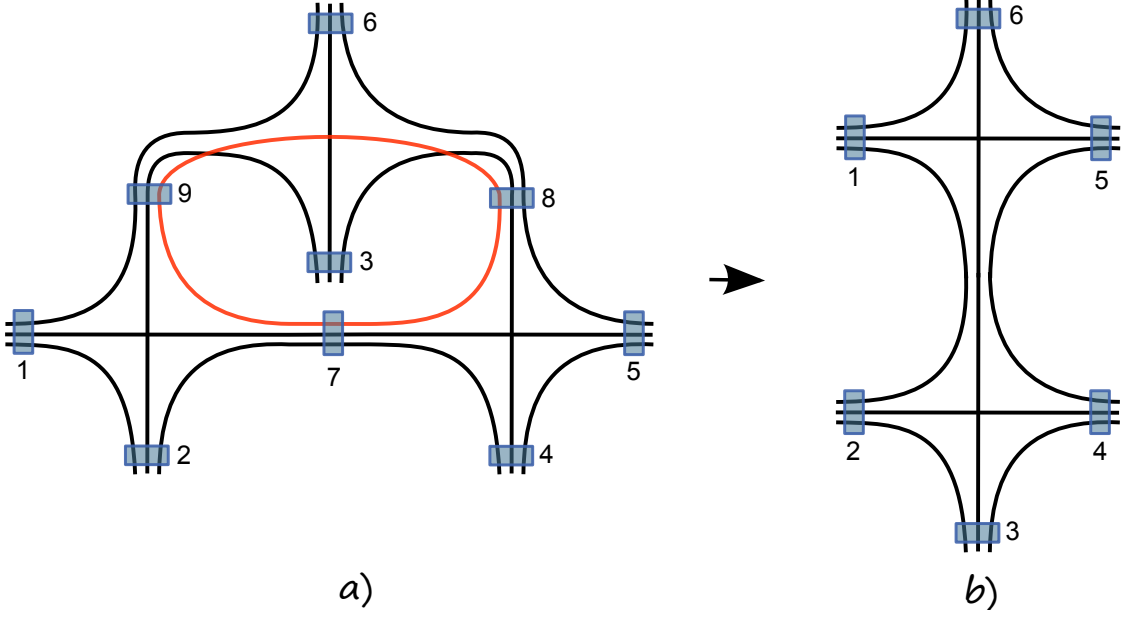


FIG. 7: a) Cable diagram for the 3-2 move. The internal loop is colored. b) After gauge-fixing projectors 7 and 9 and performing loop identity on projector 8, the diagram reduces to gluing of two tetrahedral graphs.

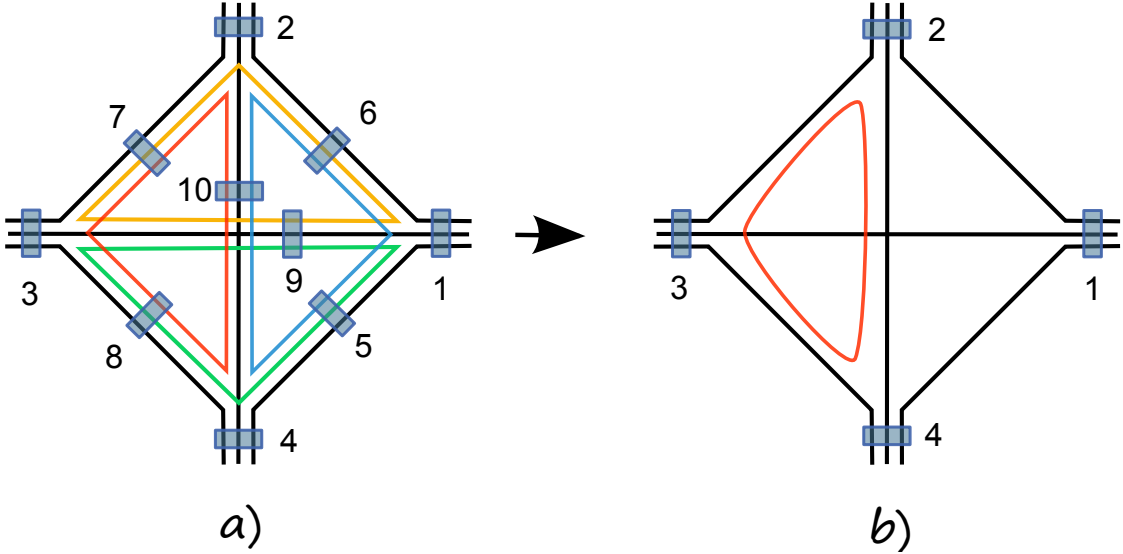


FIG. 8: a) Cable diagram for the 4-1 move. The 4 different loops are colored. b) After applying three loop identities we are left with a tetrahedral cable graph with an insertion of one loop.

Hence, we have shown that the BF partition function is invariant under the 4-1 move up to an overall divergent factor. The divergence we obtain in $SU(2)$ BF theory is exactly a $SU(2)$ delta function $\delta_{SU(2)}(\mathbb{1}) = \sum_j (2j+1)^2$. In [65] it was shown that this is the same as the volume of the $\mathfrak{su}(2)$ Lie algebra. If we put on a cut-off Λ on spins, then the divergence scales as $\sum_j (2j+1)^2 \sim \Lambda^3$. Since in 3d spin is proportional to length, we get a divergence that corresponds to the translation symmetry of placing the extra vertex inside the tetrahedron. A correct Fadeev-Popov procedure [65] divides the amplitude by exactly this divergence, so the Ponzano-Regge model is invariant

after gauge fixing under both the 3–2 and 4–1 Pachner moves. This gauge fixing procedure was subsequently refined in [71–74] to lead to a complete definition of 3 dimensional manifold invariant.

IV. PACHNER MOVES IN 4D RIEMANNIAN HOLOMORPHIC SPIN FOAM MODEL

In this section we obtain the main results of this paper. To calculate the 4d Pachner moves, we follow the strategy used in the BF case and calculate a constrained version of the loop identity, which together with gauge fixing makes this involved calculation manageable. We find, unsurprisingly, that the models in question are not invariant under Pachner moves. The difference from the BF case is the presence of mixing of strands that exchanges the trivial propagators and delta functions with more complicated operators. We discuss the possible meaning of this mixing of strands as an insertion of an operator.

A. Toy Loop

To capture the essence of the computation without too much complexity, let us start with repeating the calculation of the BF loop identity, but with the constrained propagator $P_\rho(z_i; w_i)$ (38) rather than the $SU(2)$ projector. We will follow the treatment of the loop identity from Section III D. We will thus find the loop identity for the generating functional

$$G_\tau(z_i; w_i) = e^{\tau \sum_{i < j} [z_i | z_j] [w_i | w_j]}$$

and at the end of the calculation use the homogeneity map to get the loop identity for $P_\rho(z_i; w_i)$ by changing $\tau^J \rightarrow F_\rho(J)/(J+1)!$. We also want to be able to insert a face weight, which is a function of the spin we will sum over. This face weight could be *a priori* arbitrary, but for the sake of definiteness, let us choose it to be $(2j+1)^\eta$ with $\eta \in \mathbb{R}$ being a free parameter, which keeps track of divergence properties of the Spin Foam model. The method we use allows us of course to modify the face weight to an arbitrary function of spin. To insert the face weight, we follow the calculation in BF theory and rescale the spinor in the loop by an additional factor of τ' , which will keep track of homogeneity of that specific spinor. At the end of the calculation we can restore the face weight by replacing $\tau'^{2j} \rightarrow (2j+1)^\eta$ in the series expansion. Let us now calculate the constrained loop identity:

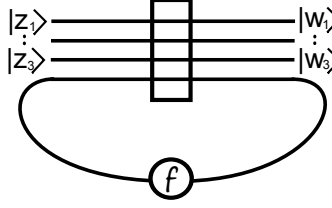
$$\int d\mu_\rho(z_4) e^{\tau \sum_{i < j < 4} [z_i | z_j] [w_i | w_j] - \tau \tau' \sum_{i < 4} \langle z_4 | z_i \rangle [w_i | z_4]} = \frac{e^{\tau \sum_{i < j < 4} [z_i | z_j] [w_i | w_j]}}{\det \left(\mathbb{1} - \frac{\tau \tau'}{1 + \rho^2} \sum_{i < 4} |w_i\rangle [z_i|] \right)}. \quad (65)$$

Unsurprisingly, we get nearly the same result as in Section III D, the difference being the additional factor of $1/(1 + \rho^2)$, which arises from the modified integration measure $d\mu_\rho(z)$. Of course, the τ also carries a hypergeometric function of ρ . We can again use the lemma III.2 to evaluate the determinant. We arrive thus at the result

$$\begin{aligned} \int d\mu_\rho(z_4) G_\tau(z_1, \dots, \tau' z_4; w_1, \dots, z_4) &= \frac{e^{\tau \sum_{i < j < 4} [z_i | z_j] [w_i | w_j]}}{1 - \frac{\tau \tau'}{1 + \rho^2} \sum_{i < 4} [z_i | w_i] + \sum_{i < j < 4} \frac{\tau^2 \tau'^2}{(1 + \rho^2)^2} [z_i | z_j] [w_i | w_j]} \\ &= e^{\tau \sum_{i < j < 4} [z_i | z_j] [w_i | w_j]} \sum_{N, M} \frac{(N + M)!}{N! M!} \left(\frac{\tau \tau'}{1 + \rho^2} \right)^{N + 2M} \left(\sum_{i < 4} [z_i | w_i] \right)^N \left(- \sum_{i < j < 4} [z_i | z_j] [w_i | w_j] \right)^M. \end{aligned} \quad (66)$$

We can now expand the exponential, combine the mixing terms and use the homogeneity map to reintroduce the face weight and the hypergeometric function of ρ . We hence find that the

constrained loop identity for $P_\rho(z_i; w_i)$ is given by

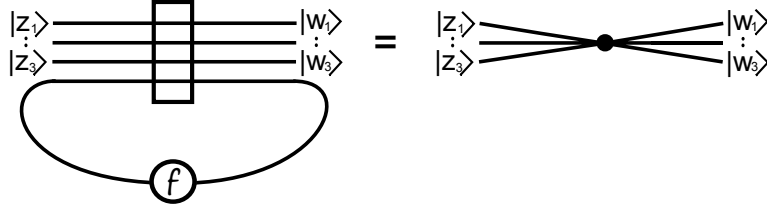


$$= \sum_{J, J'} C_\rho(J, J') \left(\sum_{i < n} [z_i | w_i] \right)^J \left(\sum_{i < j < n} [z_i | z_j] [w_i | w_j] \right)^{J'}, \quad (67)$$

with the coefficient $C_\rho(J, J')$ given by

$$C_\rho(J, J') = \sum_K (-1)^{J'-K} \frac{(J+J'-K)!(J+2J'-2K+1)^\eta F_\rho(J+2J'-2K)}{J!(J'-K)!K!(J+2J'-K+1)! (1+\rho^2)^{J+2J'-2K}}, \quad (68)$$

where $F_\rho(J) = {}_2F_1(-J-1, -J; 2; \rho^4)$. We have hence arrived at an expression very similar to the one in BF theory – we again got the trivial propagation terms $\sum_{i < 4} [z_i | w_i]$ together with additional mixing terms like $\sum_{i < j < 4} [z_i | z_j] [w_i | w_j]$. Unlike in the BF loop identity however, there is no miraculous cancellation of the $J' \neq 0$ terms, unless we choose $\rho = 0$ and $\eta = 1$, i.e. we reduce this to $SU(2)$ BF theory. Hence the way in which simplicity constraints break the topological symmetry is by introducing additional mixing terms in the loop identity. We can represent this graphically as



$$= \begin{array}{c} |z_1\rangle \\ |z_2\rangle \\ |z_3\rangle \\ |z_4\rangle \end{array} \rightarrow \bullet \leftarrow \begin{array}{c} |w_1\rangle \\ |w_2\rangle \\ |w_3\rangle \\ |w_4\rangle \end{array} \quad (69)$$

B. The Constrained Loop Identity

We are now going to see that the loop identity we need for Pachner moves is somewhat different with the one we considered in the previous section. When we glue together 4-simplices, we need to glue them along their boundaries, necessitating the gluing of two propagators, i.e. we should work with $P_\rho \circ P_\rho$, rather than a single P_ρ . The reason for this being that in our model the propagator P_ρ is inserted around each vertex and we get the composition of them along an edge. Since P_ρ is not a projector unless $\rho = 0$ we have $P_\rho \circ P_\rho \neq P_\rho$. Additionally, the loops arising in all the Pachner moves always are composed of three groups of propagators $P_\rho \circ P_\rho$, rather than the single one we have considered. Fortunately, two of these can be always gauge fixed by a proper choice of a maximal tree, so that we have to consider the loop identity shown in Fig.9. In BF theory the gauge-fixing reduces the projectors to trivial propagators $\mathbb{1}(z_i; w_i)$, so we did not have to worry about this issue.

We thus have to first find the equivalent of the trivial propagator in the constrained case, i.e. the analog of setting $g = \mathbb{1}$ in (16) to get (10) but for the propagator (38). We thus have to restore the group integration. Fortunately, by tracking homogeneity for each term, we know that

$$\frac{\left(\sum_{i < j} [z_i | z_j] [w_i | w_j] \right)^J}{J!(J+1)!} = \sum_{\sum j_i = J} \int dg \prod_{i=1}^4 \frac{[z_i | g | w_i]^{2j_i}}{(2j_i)!}. \quad (70)$$

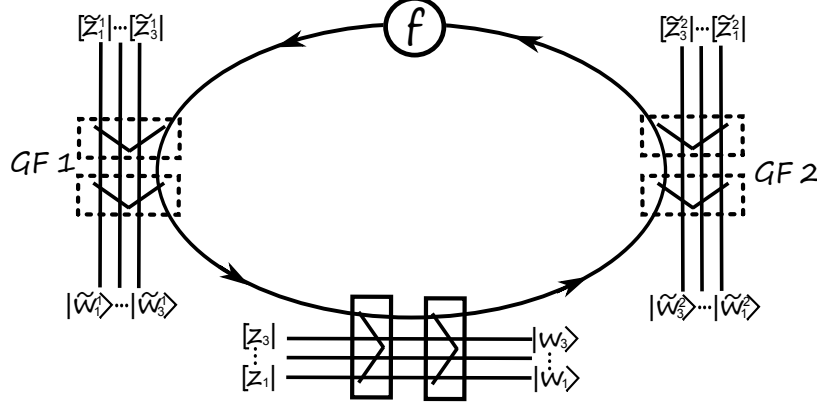


FIG. 9: Loop identity with for the constrained projector with two extra gauge fixed projectors

Setting this $SU(2)$ group element to identity and summing over all J allows us to get the partially gauge fixed propagator, which we denote $\mathbb{1}_\rho$

$$\mathbb{1}_\rho(\tilde{z}_i; \tilde{w}_i) = \sum_J {}_2F_1 \left(-\frac{J}{2} - 1, -\frac{J}{2}; 2; \rho^4 \right) \frac{(\sum_i [\tilde{z}_i | \tilde{w}_i])^J}{J!}. \quad (71)$$

Note that for the convenience of notation later, we will always add a tilde on the spinors which belong to the partially gauge fixed propagator. As in the case of the propagator, we find that setting $\rho = 0$ we recover the BF trivial propagator $\mathbb{1}(z_i; w_i)$, as we would expect. We can now use the homogeneity map to define a homogenized trivial propagator $\mathbb{1}_{\tilde{\tau}}$ as

$$\mathbb{1}_{\tilde{\tau}} = e^{\tilde{\tau} \sum_i [\tilde{z}_i | \tilde{w}_i]} \quad \text{with} \quad \tilde{\tau}^J \rightarrow F_\rho(J/2) \quad \text{for} \quad \mathbb{1}_{\tilde{\tau}} \rightarrow \mathbb{1}_\rho. \quad (72)$$

We thus have arrived at the expression for the gauge fixed propagators that are necessary for the loop identity. We will have to consider however $P_\rho \circ P_\rho$ and $\mathbb{1}_\rho \circ \mathbb{1}_\rho$, rather than single propagators, as we have mentioned above. We will thus use the following homogeneity maps: for the pair of gauge-fixed propagators we will have

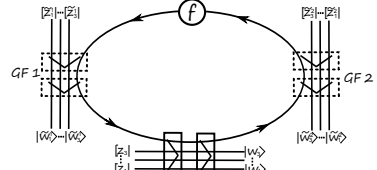
$$\mathbb{1}_{\tilde{\tau}} \circ \mathbb{1}_{\tilde{\tau}} = e^{\tilde{\tau} \sum_i [\tilde{z}_i | \tilde{w}_i]} \quad \text{with} \quad \tilde{\tau}^J \rightarrow \frac{F_\rho(J/2)^2}{(1 + \rho^2)^J} \quad \text{for} \quad \mathbb{1}_{\tilde{\tau}} \circ \mathbb{1}_{\tilde{\tau}} \rightarrow \mathbb{1}_\rho \circ \mathbb{1}_\rho, \quad (73)$$

while for the pair of propagators P_ρ we get

$$G_\tau \circ G_\tau = e^{\tau \sum_{i < j} [z_i | z_j] [w_i | w_j]} \quad \text{with} \quad \tau^J \rightarrow \frac{F_\rho(J)^2}{(1 + \rho^2)^{2J} (J + 1)!} \quad \text{for} \quad G_\tau \circ G_\tau \rightarrow P_\rho \circ P_\rho. \quad (74)$$

With this, we are ready to perform the calculation of this loop identity. The addition of the extra two pairs of gauge-fixed propagators leads to very simple contractions, using our results of spinor Gaussian integrals in the Appendix. Integrating over the three strands inside the loop leads to nearly the same calculation as in the previous section, with the difference being the addition of the trivial propagation in the extra strands connected to the gauge-fixed propagators. Using the

homogeneity map, we finally find that the constrained loop identity is given by



$$\begin{aligned}
 &= \sum_{A,B,J,J'=0}^{\infty} \frac{N(A,B,J,J',\rho)}{A!B!J!J!} \times \\
 &\times \underbrace{\left(\sum_{i=1}^3 [\tilde{z}_i^1 | \tilde{w}_i^1] \right)^A}_{GF1} \underbrace{\left(\sum_{i=1}^3 [\tilde{z}_i^2 | \tilde{w}_i^2] \right)^B}_{GF2} \underbrace{\left(\sum_{i=1}^3 [z_i | w_i] \right)^J}_{\text{Trivial projection}} \underbrace{\left(\sum_{i < j < 4} [z_i | z_j] [w_i | w_j] \right)^{J'}}_{\text{Mixing terms}},
 \end{aligned} \tag{75}$$

with the coefficient $N(A,B,J,J',\rho)$ given by

$$\begin{aligned}
 N(A,B,J,J',\rho) &\equiv \sum_{K=0}^{J'} \frac{J'!(J+K)!(J+2K+1)^\eta}{K!(J'-K)!(J+J'+K+1)!} \frac{(-1)^K}{(1+\rho^2)^{(A+B+12K+7J+2J')}} \times \\
 &\times F_\rho^2(J+J'+K) F_\rho^2((A+J)/2+K) F_\rho^2((B+J)/2+K),
 \end{aligned}$$

where we have defined $F_\rho(J) \equiv {}_2F_1(-J-1, -J; 2; \rho^4)$. The variables $|\tilde{z}_i^1\rangle, |\tilde{w}_i^1\rangle$ appear in the strands attached to the first gauge fixing term, similarly $|\tilde{z}_i^2\rangle, |\tilde{w}_i^2\rangle$ appear in the second gauge fixing, while $|z_i\rangle, |w_i\rangle$ are labelled for the strands we haven't gauge fixed. The face weight coupling constant η should be fixed by requirements of divergence, which we will discuss in a later section. A more detailed calculation of this loop identity can be found in the Appendix.

Even though the expression in Eq.(75) has a few layers of summations like a Russian nesting doll and the coefficients look complicated, the physical meaning behind the expression is quite clean – up to a weight, we get the trivial propagation, like in BF theory, but we also get additional mixing terms for $J' \neq 0$. We will study the properties of this identity in section V A.

For the purpose of calculating the 4-dimensional Pachner moves, it will be convenient to again define an exponentiated expression for this loop identity, which can then be transformed into the proper expression by the homogeneity map. Before using the homogeneity map in Eq. (75), we would have an expression purely in terms of τ 's that can be exponentiated. We hence define the exponentiated loop identity to have the following very simple form:

$$L_\tau(z_i, w_i; \tilde{z}_i^1, \tilde{w}_i^1; \tilde{z}_i^2, \tilde{w}_i^2) = \exp \left(\sum_{i=1}^3 \tilde{\tau}_1 [\tilde{z}_i^1 | \tilde{w}_i^1] + \tilde{\tau}_2 [\tilde{z}_i^2 | \tilde{w}_i^2] + \tau_N [z_i | w_i] + \tau_M \sum_{i < j < 4} [z_i | z_j] [w_i | w_j] \right). \tag{76}$$

The full loop identity can then be recovered through the following homogeneity map:

$$\tau_N^J \tau_M^{J'} \rightarrow \sum_{K=0}^{J'} \frac{(-1)^K (J+K)! J!}{K! (J'-K)!} (J+2K+1)^\eta \tau^{J'-K} \left(\frac{\tilde{\tau}_1 \tilde{\tau}_2 \tau}{(1+\rho^2)^3} \right)^{J+2K} \tag{77}$$

and the $\tilde{\tau}$'s and τ keep track of the F_ρ factors according to the rules given in Eq. (73) and Eq. (74).

C. Computing Pachner Moves with Simplicity Constraints

In this section we compute all the Pachner moves in the 4-d holomorphic Spin Foam model based on the techniques we have developed in the previous sections. All these moves are based on

the configurations of 6 vertices ($ABCDEF$). In the following we adopt the following notation: a simplex A indicates the 4-simplex opposite to the vertex A , i.e. it is composed by $[BCDEF]$. AE indicates the tetrahedron $A \cap E$ composed of the vertices $[BCDF]$, with vertex A and E removed from the triangulation. Triangle ABD indicates the one composed by $[CEF]$. Also in order to keep track of which vertex is “active”, i.e. dual to a 4-simplex and which vertex is “inactive”, i.e. not dual to a 4-simplex, we introduce a distinction in our notation: an upper case letter $A, B \dots$ denotes an active vertex, while a lower case letter $c, d \dots$ denotes an inactive vertex.

1. 3-3 move

According to these conventions the move 3-3 corresponds to

$$ABCdef \rightarrow abcDEF.$$

The 3-3 move is shown as Fig.10. In the first figure the 4-simplices A, B, C are sharing the blue triangle. After the move the configuration is changed into three 4-simplices D, E, F which share the green triangle.

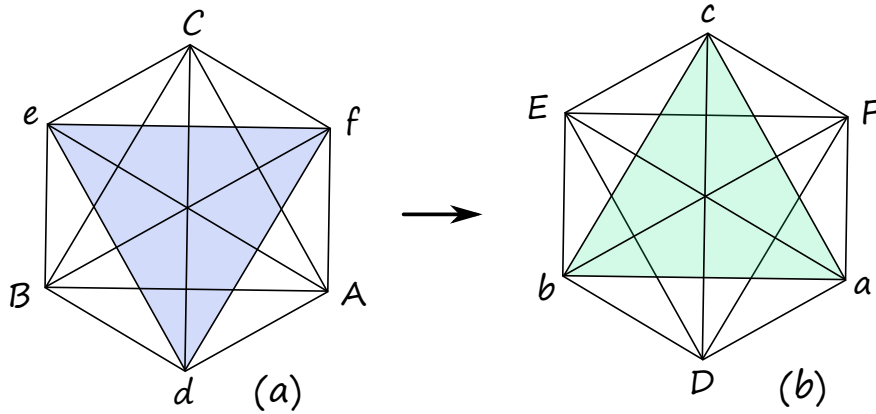


FIG. 10: Triangulations for the 3-3 move.

The corresponding cable diagram is shown in Fig.11. The various colours of strands in the graph are used to indicate the different positions of triangles. The blue loop to be integrated out corresponds to the triangle ABC . The purple strands in (a) for example are dual to the triangles $Adf \subset A$, $Bde \subset B$, $Cef \subset C$ and they run from the tetrahedra $Af \rightarrow Ad$, $Bd \rightarrow Be$, $Ce \rightarrow Cf$. After performing the 3-3 Pachner move, the same triangles (still indicated by the purple strands) are no longer shared by two tetrahedra within a given 4-simplex. They become commonly shared by tetrahedra belonging to the three different 4-simplices: $aDF \subset (D \cap F)$, $bDE \subset (D \cap E)$, $cEF \subset (E \cap F)$. The same happens to the black strands, whereas the opposite happens for the red and light blue strands. In summary, on one hand, due to the 3-3 move from (a) to (b), the red and light blue strands, shared between different simplices in (a) become unshared strands which belong to one simplex in (b). On the other hand, the unshared strands (the black and purple strands) in a become the commonly shared ones in (b). The dark blue loop and the green loop correspond to faces which are dual to the internal triangles ABC and DEF respectively.

To compare the partition function/amplitudes between the configurations (a) and (b), we need to integrate out the shared loop on both sides. Based on the discussion in section IIIB, we can gauge fix two out of three pairs of the constrained propagators around the loop by a choice of a maximal tree in a way that leaves the amplitude invariant. We then need to apply only once the

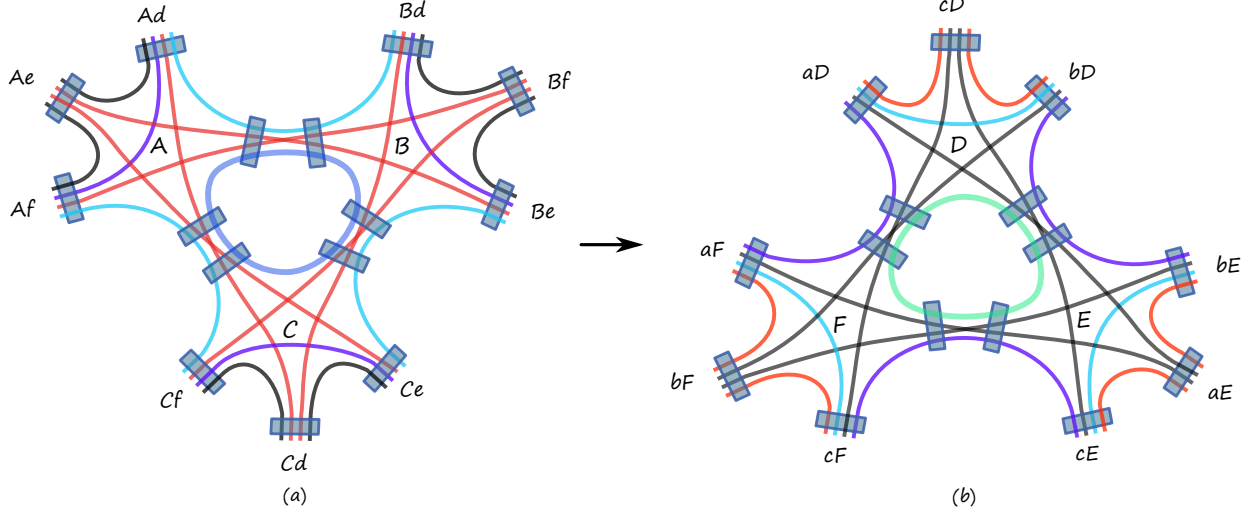


FIG. 11: Cable diagram for the 3-3 move $ABCdef \rightarrow abcDEF$.

constrained loop identity which we obtained in the previous section to complete the 3-3 Pachner move. In order to do so, it is important to introduce some notation for the spinors. Let us describe the parametrization of $(a) = (ABCdef)$. For each 4-simplex $\alpha \in \{A, B, C\}$ we need to introduce a collection of spinors associated with each strand within that 4-simplex. Each strand carries a label which corresponds to a pair of tetrahedra $\alpha\beta$ sharing a face. Within A we have two types of tetrahedra: three external ones Ad, Ae, Af and two internal ones AB, AC . The strands run either between two internal tetrahedra or from one internal to one external tetrahedron. Accordingly, we label the external strands by boundary spinors $z_\gamma^{\alpha\beta}$ where $\alpha \in \{A, B, C\}$, $\beta \in \{d, e, f\}$, $\gamma \in \{A, B, C, d, e, f\}$ for (a) in Fig.11, and $\alpha \in \{D, E, F\}$, $\beta \in \{a, b, c\}$, $\gamma \in \{a, b, c, D, E, F\}$ for (b) . $\alpha\beta$ are the indices labeling boundary tetrahedra, and $z_\gamma^{\alpha\beta}$ indicate boundary spinors. The boundary propagators are then labeled as $P_\rho(z_\gamma^{\alpha\beta}; w_\gamma^{\alpha\beta})$.

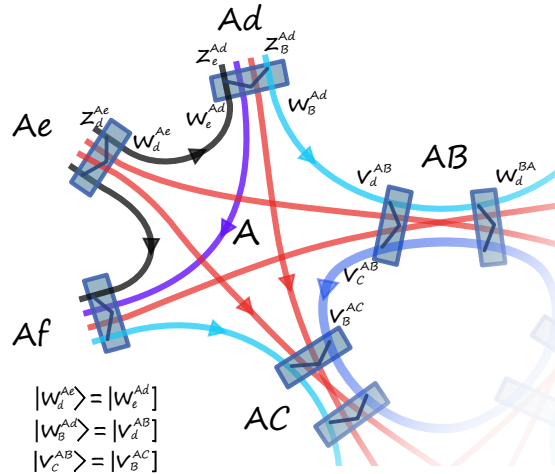
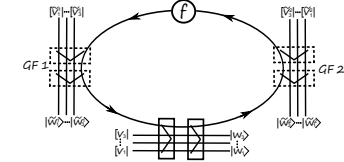


FIG. 12: Zoomed in part of the cable diagram for the 3-3 move with some of the labels and contractions of spinors explicitly written down.

Let us label the internal pairs of propagators by $P_\rho \circ P_\rho(v_\gamma^{\alpha\alpha'}, w_\gamma^{\alpha'\alpha})$, where $\alpha, \alpha' \in \{A, B, C\}$ for (a) and $\alpha, \alpha' \in \{D, E, F\}$ for (b) . We need to contract these spinors with the spinors $w_\gamma^{\alpha\beta}$ of the

external propagators. An example of this is shown in Fig. 12 with all the labels and orientations written explicitly of a part of (a). The contractions are done according to the orientations of strands, and for example we have $|w_B^{Ad}\rangle = |v_d^{AB}\rangle$. In summary, the amplitude is constructed from $z_\gamma^{\alpha\beta}$ and $w_\gamma^{\alpha\beta}$ for the external propagators and on $w_\gamma^{\alpha\alpha'}, v_\gamma^{\alpha\alpha'}$ for the internal ones. The amplitude is obtained then after integration over the internal spinors after imposing the contractions, thus becomes a function of $z_\gamma^{\alpha\beta}$ only.

We thus find that the amplitude for three 4-simplices combined as in Fig.11 can be written as

$$\mathcal{A}_3(z_\gamma^{\alpha\beta}) = \int \prod_{all} d\mu_\rho(v) d\mu_\rho(w) \prod_{\alpha\beta} P_\rho(z_\gamma^{\alpha\beta}; w_\gamma^{\alpha\beta}). \quad (78)$$


The spinors of the three internal propagators which share a loop are labeled by v and w and each of them is contracted with different boundary constrained propagators, with the gluing depending on the orientation of the graph.

The crucial difference between amplitude (a) and (b) is that the non-trivial coefficient $N(J, J', A, B, \rho)$ of Eq.(75) encodes the spin information of different strands. In (a), the coefficient N encodes the spin information of the blue and red strands in one configuration, while in (b) it encodes the spin of the black and purple strands. Unless the corresponding boundary spins are chosen to be the same, the 3-3 move cannot be invariant.

It is thus very easy to see where the topological invariance of BF theory is broken. Let us come back to BF theory and look at the 3-3 move. The BF loop identity (57) does not have any factor depending on spins and hence gives a trivial equality, as the diagrams in Fig. 13 are combinatorially equivalent. Thus for BF theory, the partition function/amplitudes are invariant under 3-3 move.

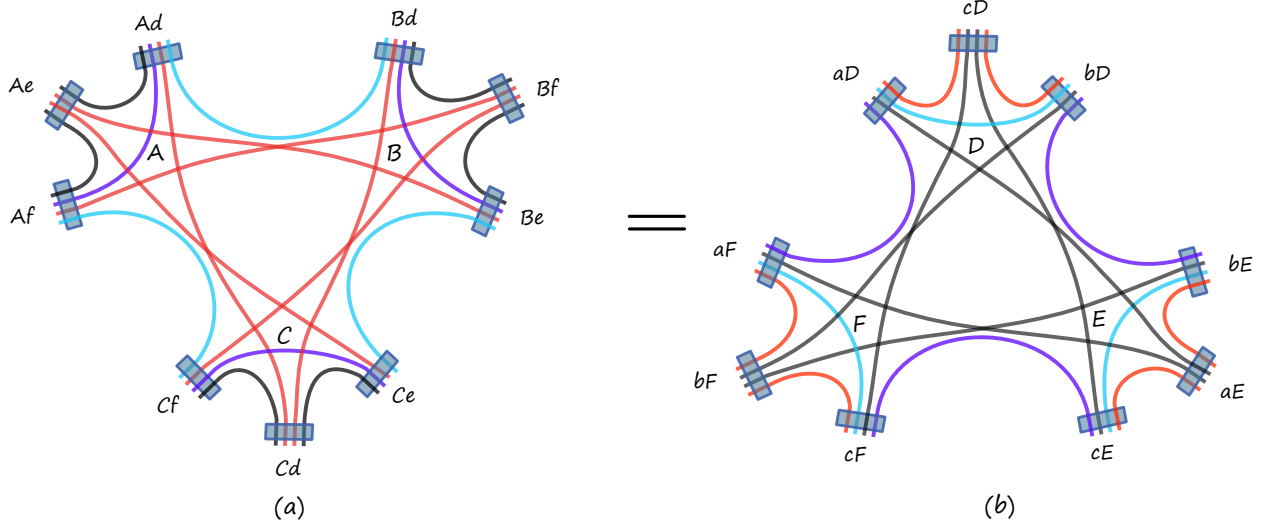


FIG. 13: For 4-d BF theory, after integrating out the middle loops in the 3-3 move, the rest of the strands are combinatorially equivalent.

2. 4-2 move

The 4-2 move $ABCDef \mapsto abcdEF$ is shown in Fig.14. In (a), four 4-simplices A, B, C, D are sharing 6 tetrahedra. After removing four triangles (or four loops in the dual cable graph) and changing the combinatorial structure, the four 4-simplices are rearranged in two 4-simplices E, F glued by one tetrahedron. The corresponding cable diagram of the four 4-simplices is shown in Fig.15.

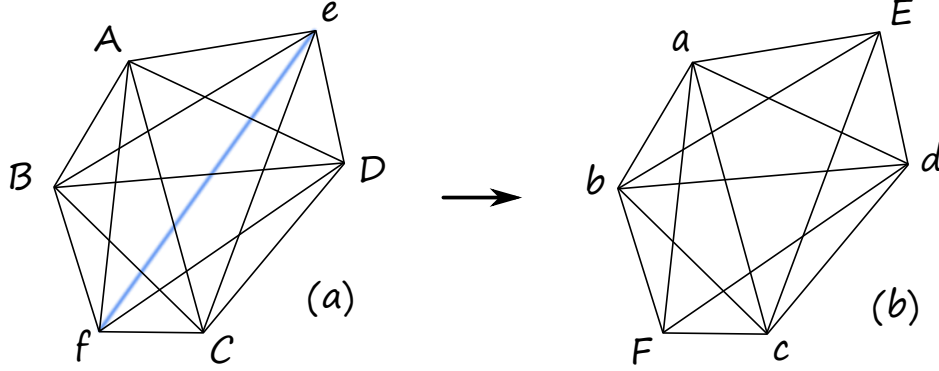


FIG. 14: Triangulations for the 4-2 move.

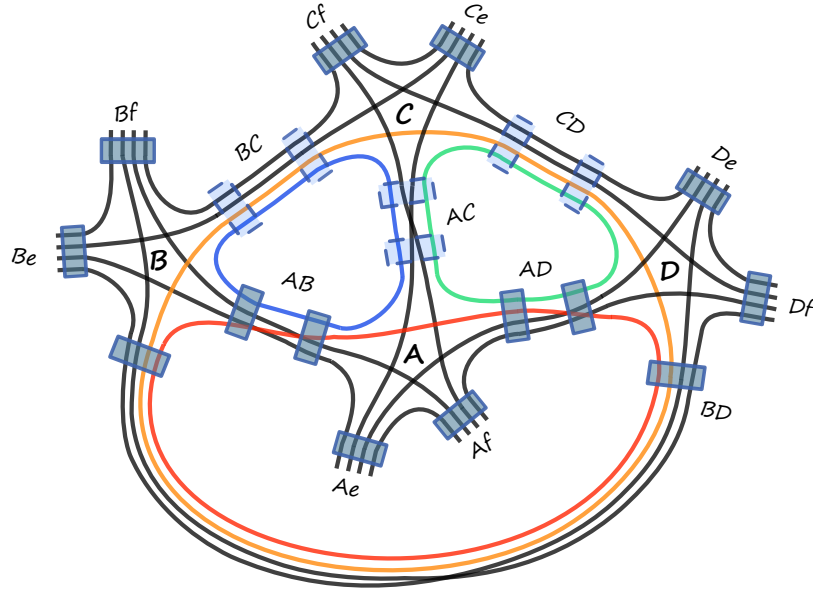


FIG. 15: Cable diagram for the 4-2 move with gauge fixing along BC, AC, CD .

We can perform gauge fixing of this graph by choosing vertex C as the root of the maximal tree in such a way that we can gauge fix 3 couples of propagators BC, AC, CD . This allows us to apply the constrained loop identities Eq.(75) to three of the four loops. More specifically, we can apply the constrained loop identity to the propagators (AB, BC, CA) to drop the blue loop, then apply it to the propagators (AC, CD, DA) to integrate the green loop and propagators (BC, CD, DB) to remove the big yellow loop. This results in integrating out all couples of constrained propagators, and hence we are left with one last (red) loop, which is mixed with the external strands, as can be seen in Fig.16.

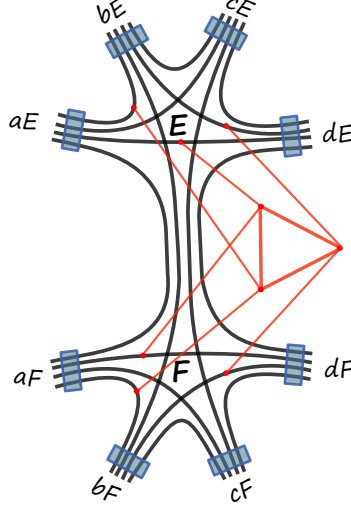


FIG. 16: Performing the calculation we get a configuration of two 4-simplices with a nonlocal gluing.

Note, that we have applied the three loop identities, but the last loop is left without any extra group averaging. Similar to the case of the loop identity, we have to add in a face weight for this last loop. We will do so again by inserting a factor of τ' on one of the strands of the left-over loop (say the red strand for edge AD), so that we can use homogeneity map $\tau'^{2j} \rightarrow (2j + 1)^\eta$.

Similar as in the previous section, we will denote the spinors on the boundary as z , and spinors in the bulk as w and v with indices labeling the propagator and the strand they belong to. Each spinor carries three indices: $z_\gamma^{\alpha\beta}$ with indices α labeling the 4-simplex, $\alpha\beta$ labelling the tetrahedron they belong to, γ labelling which strands they represent. With assuming a specific orientation of the graph as $C \rightarrow A, C \rightarrow B, C \rightarrow D, A \rightarrow B, D \rightarrow A, D \rightarrow B$ ⁴, the amplitude in terms of the exponentiated loop identity Eq.(76) is given then by

$$\begin{aligned} \mathcal{A}_{4-2}^\tau(z_\gamma^{\alpha\beta}) &= \int \left\{ \prod_{\text{all}} d\mu_\rho(v) d\mu_\rho(w) \right\} \prod_{\alpha\beta} P_\rho(z_\gamma^{\alpha\beta}; w_\gamma^{\alpha\beta}) \cdot \exp \left[\sum_{\sigma i} \tilde{\tau}_{\sigma C} [\tilde{v}_i^{C\sigma} | \tilde{w}_i^{\sigma C}] \right] \\ &\times \exp \left[\sum_{\mu\nu} (\tau_N^{\mu\nu} \sum_j \alpha_j^{\mu\nu} [v_j^{\mu\nu} | w_j^{\nu\mu}] + \tau_M^{\mu\nu} \sum_{j < k} \alpha_j^{\mu\nu} [w_j^{\nu\mu} | w_k^{\nu\mu}] [v_j^{\mu\nu} | v_k^{\mu\nu}]) \right]. \end{aligned} \quad (79)$$

For the external propagators $\alpha \in \{A, B, C, D\}$ and $\beta \in \{e, f\}$ label the tetrahedron, while $\gamma \in \{A, B, C, D, e, f\}$ labels the strands in each tetrahedron. For internal gauge fixed propagators, $\sigma \in \{A, B, D\}$, $i \in \{e, f\}$, and for the non-gauge fixed propagators, $\mu\nu \in \{AB, AD, BD\}$, $j, k \in \{e, f, r\}$, where r indicates the red strand of the left-over loop. We define $\alpha_j^{\mu\nu}$ as

$$\alpha_j^{\mu\nu} = 1 + \delta_{AD}^{\mu\nu} \delta_j^r (\tau' - 1) \quad (80)$$

for keeping track of the homogeneity factor for the face weight of the last loop.

The equation (79) gives a compact and explicit expression for the amplitude associated with the 4-2. It is obtained by using the exponentiated loop identity Eq.(76), which then can be transformed using the homogeneity map to obtain the full expression after performing all of the contractions of spinors and all the Gaussian integrals. The homogeneity maps we need to apply to

⁴ When one reverses the orientation of one propagator, the corresponding $[v|w] \rightarrow [w|v] = -[v|w]$

this expression to get the full result were defined in Eq. (73) for the $\tilde{\tau}$, in Eq.(77) for τ_N and τ_M and the homogeneity map for τ' is $\tau'^{2j} \rightarrow (2j+1)^\eta$. The calculation can be straightforwardly done, but the resulting expression itself is a complicated, one with lots of mixed strands that is difficult to manipulate. The integrals also contain potential divergences that have to be taken care of. We will delay the discussion of the resulting expression and the significance of the mixing terms until the next section, as we first encounter a similar behaviour for the 5–1 Pachner move as well. Here in the expression Eq.(79), we intentionally leave the last red loop unintegrated to pave the way for truncation in section V.

3. 5–1 move

We now calculate the 5–1 Pachner move. The 5–1 move corresponds to a change of a configuration of five 4-simplices sharing an internal vertex into a single 4-simplex by removing the common vertex, see Fig. 17.

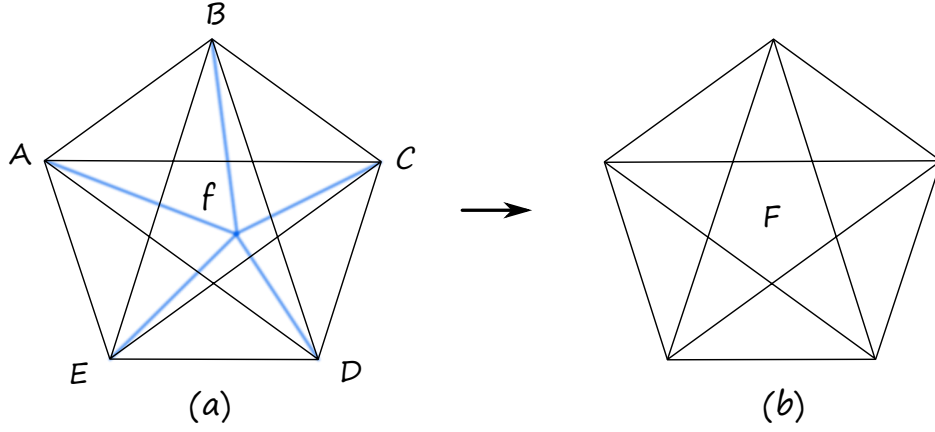


FIG. 17: Triangulations for the 5–1 Pachner move.

The cable diagram for this move can be seen in Fig. 18. We have a total of 10 loops and 10 pairs of constrained propagators inside the bulk of the graph. Even though there is an increase in complexity, compared to the 4–2 move, the calculation will go over in nearly the same way. We start by choosing a maximal tree in the diagram, which allows us to gauge fix 4 of the pairs of propagators. A careful choice of this tree corresponds to a root at one of the 4-simplices and allows us to apply loop identities to 6 of the loops, leaving us with 4, as can be seen in Fig. 19.

We can write the amplitude for the 5–1 move using the exponentiated loop identity Eq.(76) as in the case of the 4–2 move. We will again have to add the face weights for the last four loops by adding factors of τ' . The expression for the full Pachner move then would be obtained by applying the homogeneity map to the resulting power series. We keep to the notation of inside spinors being w and v labeled by the strands and propagators they belonged to. With assuming the orientation of the graph as $E \rightarrow A, E \rightarrow B, E \rightarrow C, E \rightarrow D$, the amplitude in terms of boundary spinors z is formally given then as

$$\begin{aligned} \mathcal{A}_{5-1}^\tau(z_\gamma^{\alpha f}) &= \int \left\{ \prod_{\text{all}} d\mu_\rho(v) d\mu_\rho(w) \right\} \prod_\alpha P_\rho(z_\gamma^{\alpha f}; w_\gamma^{\alpha f}) \cdot \exp \left[\sum_\beta \tilde{\tau}_{E\sigma} [\tilde{v}^{E\sigma} | \tilde{w}^{\sigma E}] \right] \\ &\times \exp \left[\sum_{\mu\nu} (\tau_N^{\mu\nu} \sum_i \beta_i^{\mu\nu} [v_i^{\mu\nu} | w_i^{\nu\mu}] + \tau_M^{\mu\nu} \sum_{i<j} \beta_i^{\mu\nu} [w_i^{\nu\mu} | w_j^{\nu\mu}] [v_i^{\mu\nu} | v_j^{\mu\nu}]) \right], \end{aligned} \quad (81)$$

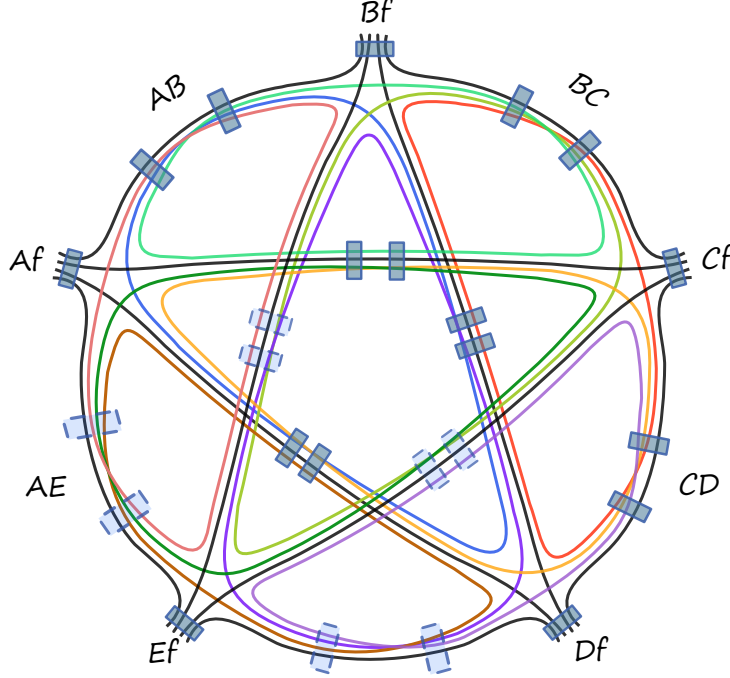


FIG. 18: Cable diagram for the 5-1 move. The loops inside are colored.

where the indices run over the following ranges: $\sigma \in \{A, B, C, D\}$, $\mu\nu \in \{AB, AC, AD, BD, BC, CD\}$, $i, j \in \{f, b, r, y, g\}$, where b, r, y, g indicates the blue (ABD), red (BCD), yellow (ACD), green (ABC) strands of the left-over loops respectively, and f indicates the black strands which compose the simplex F after the move. The external propagators $P_\rho(z_\gamma^{\alpha f}; w_\gamma^{\alpha f})$ are defined the same way as in previous sections, namely $\alpha \in \{A, B, C, D, E\}$ labels the simplices in which the boundry tetrahedra belong to, and γ labels the strands in each tetrahedra. The coefficients $\beta_i^{\mu\nu}$ that keep track of homogeneity of the face weights are defined this time as

$$\beta_i^{\mu\nu} = 1 + \delta_{AD}^{\mu\nu} \delta_i^y (\tau'_y - 1) + \delta_{AC}^{\mu\nu} \delta_i^g (\tau'_g - 1) + \delta_{AB}^{\mu\nu} \delta_i^b (\tau'_b - 1) + \delta_{BC}^{\mu\nu} \delta_i^r (\tau'_r - 1). \quad (82)$$

The formal expression of 5-1 is of similar structure as the 4-2 move, with the difference being the range of the indices due to bigger number of loops and propagators. The expression (81) is relatively compact for such a complicated calculation and it contains all the information necessary to evaluate the amplitude after the Gaussian integrations are performed. In order to do so we just need to specify is the homogeneity map

$$H_{5-1}[\mathcal{A}_{5-1}^\tau] = \mathcal{A}_{5-1}. \quad (83)$$

The 5-1 homogeneity map H_{5-1} is given by the composition of :

$$\begin{aligned} \tau_N^{\mu\nu J} \tau_M^{\mu\nu J'} &\rightarrow \sum_K \frac{(-1)^{J'-K} (J+J'-K)! J'!}{K! (J'-K)!} (J+2J'-2K+1)^\eta \tau_{\mu\nu}^K \left(\frac{\tilde{\tau}_{E\mu} \tilde{\tau}_{E\nu} \tau_{\mu\nu}}{(1+\rho^2)^3} \right)^{J+2J'-2K} \\ \tau_{\mu\nu}^J &\rightarrow \frac{F_\rho(J)^2}{(1+\rho^2)^{2J} (J+1)!}, \quad \tilde{\tau}_{E\sigma}^J \rightarrow \frac{F_\rho(J/2)^2}{(1+\rho^2)^J}, \quad \tau_i'^{2j} \rightarrow (2j+1)^\eta, \end{aligned} \quad (84)$$

with $F_\rho(J)$ previously defined as the hypergeometric function $F_\rho(J) = {}_2F_1(-J-1, -J; 2; \rho^4)$. The same map can be used to find the full expression for the 4-2 Pachner move as well. The Gaussian integrals for the last four loops can be performed explicitly. Using the results from [24], we can

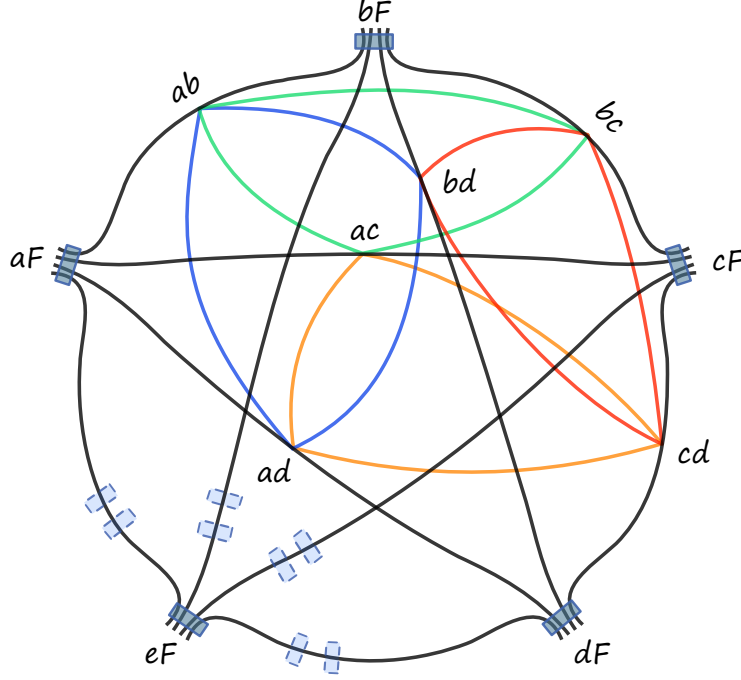


FIG. 19: Gauge-fixing 4 strands allows to apply loop identities 6 times, leaving the 4 colored loops.

write this as an inverse of a determinant of a large matrix. We leave these integrals undone however to make the truncation procedure in the next section more clear.

Let us now try to understand our result. In BF theory the 5–1 Pachner move would lead to 4 decoupled loops, each giving a factor of a $SU(2)$ delta function evaluated at identity. This would correspond to setting all the τ_{MS} to 0 and all the other τ s to 1 in our expression. For the constrained propagator, as in the previous case of the 4–2 move, the loops inside are coupled to each other and to the strands of the boundary spinors. This means that as expected the spin foam model we consider is not invariant under both the 4–2 and 5–1 Pachner moves. It is natural to conjecture here, that this would be the case for the other spin foam models as well.

The new feature of the model is the mixing between internal loops and external edges that creates a coupling between all the different strands not present in the original form of the vertex amplitude.

Let us try to study this mixing in some more detail. By splitting the 6-valent vertices in the loops, as in Fig. 20, it is obvious that we can try to interpret these coupled loops as an insertion of an operator. The connections between loops and the boundary spinors corresponds to gauge invariant operators inserted inside the 4-simplex amplitude. It is well known that such operators can be expressed as a sum of grasping operators [67].

In the holomorphic context these operators are due to the insertions of the $SU(N)$ operators [17], from which all geometrical operators are made. The insertion of Wilson loops and the action of $SU(N)$ operators are two sides of the same coin [68] – they are constructed from the same type of gauge-invariant observables, which in our language are the products $[z|w\rangle$ and $\langle z|w\rangle$. The operators we get for the 4–2 and 5–1 moves can be thus thought as an exponentiated combination of $SU(N)$ grasping operators and Wilson loops. Iteration of 5-1 moves leads to a new kind of loop expansion, reminiscent of higher order diagrams in perturbative quantum field theory. It might be interesting to flesh out more this correspondence and understand if this series converges to some interesting object. We leave this question for future work since this requires to first disentangle the divergent

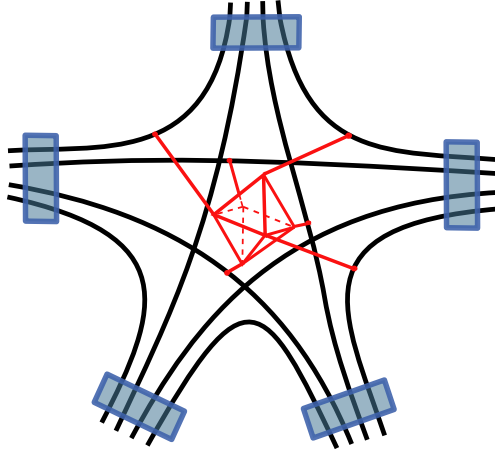


FIG. 20: Performing the calculation we get a 4-simplex with an insertion of a nonlocal operator.

part from the part that purely acts as grasping and leads to mixing of strands. We will now try a different approach to understanding these operators.

V. TOWARDS COARSE GRAINING

In the previous section we have seen that the mixing of strands could be understood as the insertion of a $SU(N)$ grasping operator. In this section we mainly focus on the 5–1 move. This move can be understood as a coarse graining move which maps one choice of the vertex amplitude to another one obtained after coarse graining. All the other coarse graining moves have to be built out of non-trivial combinations of 3–3, 4–2 and 5–1 moves. As we have shown that 5–1 move generates non-local couplings via the mixing terms, similarly to what happens in Real Space Renormalization Group calculations. Remarkably it turns out that the mixing terms are clearly subdominant. This motivates a truncation scheme in which we keep only the non-mixing terms in the 5–1 move leading to a specific renormalisation scheme for the vertex amplitude. This is what we analyse in this section.

A truncation scheme is usually associated with a choice of what are the relevant and irrelevant couplings. In the usual setting this choice is tied up with the assumptions of locality but also has to be compatible with the symmetries like Lorentz invariance and eventually should be compatible with unitarity. These concepts need to be replaced by others in the case of Spin Foam renormalisation. The current Spin Foam models, including the holomorphic one we study here, are defined in such a way that they possess the correct leading semi-classical behaviour at the level of a single 4-simplex. In hopes of defining a continuum theory down the line, the requirement of correct asymptotics should be kept unchanged at each step of truncation in the coarse graining procedure. Apart from this requirement, the only other one that is obvious is the preservation of gauge symmetries. In the next subsection, we will see that a natural truncation scheme does seem to exist for the Pachner moves already at the level of the constrained loop identity and it preserves the above requirements.

In order to successfully coarse grain the non-local operators in the Pachner moves, we need to understand and deal with their divergences, which we study in section VB. It is important to appreciate that the divergences in the 5–1 move are welcomed in Spin Foam models, since ultimately we would like to understand them as coming from a left over of diffeomorphism invariance. More precisely they should represent a translation symmetry of the internal vertex, that should be

removed by some appropriately defined Fadeev-Popov gauge-fixing procedure, similarly to what has been achieved in 3d [65]. It is natural in our context, to control the presence of potential divergences by introducing parameters like η determining the strength of the face weights and absorb the divergence into them (and perhaps into the other coupling constants already present, like ρ , the Newton constant G_N together with a cosmological constant Λ , or even the τ parameters that we treated so far as book-keeping parameters).

After having understood the truncation and divergences, we have to perform the renormalization step, which entails absorbing the relevant part of the operator into the definition of the constrained projector. This define for us a flow $P_\rho \rightarrow \tilde{P}_\rho$ in the space of constrained propagators. We leave the detailed study of this last step to future investigations.

It is interesting to note that besides the truncation we perform, we could also study the effect of the insertion of the mixing terms which are subleading contributions. For the 5–1 Pachner move, we could in principle integrate out the non-local operator. Once the divergence is removed the effect of the mixing terms leaves us with an amplitude that is more involved than a simple 4-simplex graph. It corresponds to a more general structure of all strands being mixed in the middle of the vertex, giving rise to higher-valent intertwiners. This suggests that the additional contributions would allow the theory to flow to higher-valent vertex amplitudes.

A. Truncation of the loop identity

In this section we introduce a truncation scheme for the Pachner moves, that will ultimately allow us to define the renormalization flow. The expression for the 5–1 Pachner move in Eq.(81) is very compact, but requires us to perform many extra integrations over spinors, each of which in itself is straightforward, but the resulting answer is rather long. To simplify the discussion, let us drop the dependence on the external spinors, which corresponds to setting the boundary spins to zero. As we will discuss in the next section, this selects out the most divergent part of the Pachner move. With this simplification, we can use the techniques introduced in [24] and perform all of the spinor integrals immediately, with the result being again the inverse of a determinant. The power series expansion is however very large, depending on the order of $\mathcal{O}(150)$ sums over integers. Nonetheless, its structure is simple – it is a large summation of a product of six functions $N(J, A, B, J', \rho)$ defined in the constrained loop identity in Eq.(75). Thus, instead of trying to truncate the whole 5–1 Pachner move, which is a daunting task, first we can simplify the problem by just studying the properties of a single constrained loop identity – a much more tractable problem.

Let us then take a look at the constrained loop identity. Recall that in section IV B , after we integrated out the loop, additional mixing terms appeared, which were not there in BF theory and which seem to be non-geometrical. We can analyze Eq.(75) to see how much these extra terms contribute to the amplitude. The mixing terms are characterized by their total spin J' in Eq.(75). The larger J' is, the higher order polynomials of complicated mixings appear. The mixed strands disappear only when $J' = 0$.

Let us look at the large spin behaviour first. As an illustration, the Fig. 21 presents logarithmic plots for the coefficient function $N(J, A, B, J', \rho)$ when J, A, B are universally large (as an example, we set them to 100, but it can be any large enough number), while J' picks small values $J' \in \{0, 1, 2\}$. We can observe that for any $\rho \in [0, 1]$, $N(J' = 0)$ is at least more than J times larger than the next order $N(J' = 1)$, which is also approximately more than J times larger than the next order $N(J' = 2)$. Actually, we can plot the ratio between the coefficient of the first term $N(J' = 0)$ and the sum of a few subleading coefficients $\sum_{J'=1}^{10} N(J')$ in Fig.22 as a function of ρ . When $\rho = 0$, the expression converges to the behaviour of BF theory, $N(J, A, B, 0, 0) = 1$ and

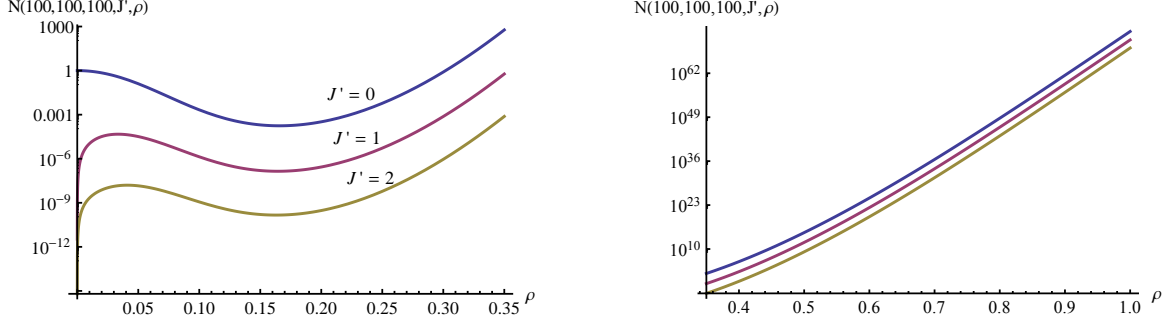


FIG. 21: Logarithmic plots for the coefficient N when $J = A = B = 100$ and face weight scaling is $\eta = 1$. The blue, red, yellow lines correspond to $J' = 0, 1, 2$ respectively.

$N(J, A, B, J', 0) = 0$ for any $J' \neq 0$, as desired. For $\rho \neq 0$, we get a smooth deformation of the BF result, with a similar behaviour, in the sense that the constrained loop identity is dominated by the $J' = 0$ term. The smaller the ρ , the more dominating the unmixed term is. The same behavior holds when spins are large but not uniformly large – the constrained loop identity is always dominated by the terms of $J' = 0$.

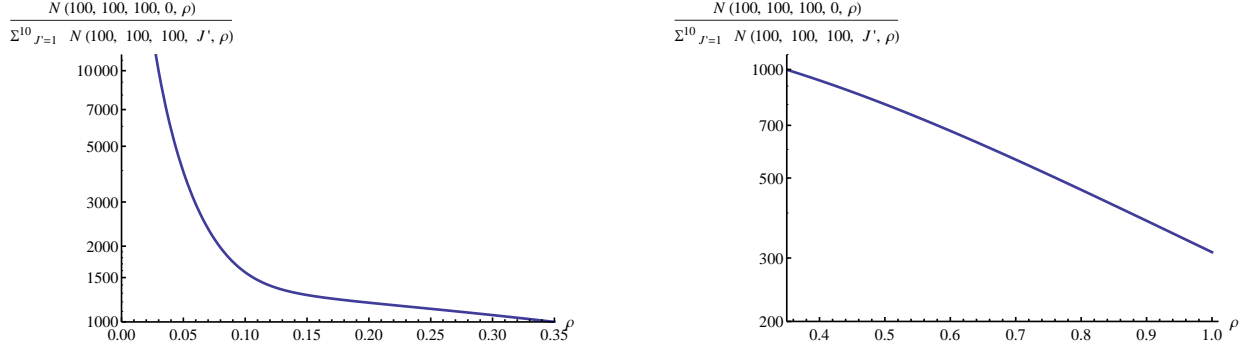


FIG. 22: Plots of the ratio between $N(J' = 0)$ and the sum of subleading coefficients $\sum_{J'=1}^{10} N(J')$ with $J = A = B = 100$ and face weight scaling $\eta = 1$.

What about the case when the spins are not large? The plots in Fig.23 illustrate that actually the $J' = 0$ terms are still dominating even when the spins J, A, B are small. This means that the dominance of $J' = 0$ terms surprisingly holds not only for large spins, but also for the small ones, even though the suppression is less pronounced compared with large spins cases. For small spins with the value of $\rho \rightarrow 1$, the dominance of $J' = 0$ term is the least pronounced but still valid.

All of these results so far have been for the choice of face weight corresponding to $\eta = 1$. One could worry that perhaps the dominance of $J' = 0$ fails for bigger face weights. We find however that the increasing of the face weight η makes the effect stronger, as it is illustrated for small spins in the Fig.24.

We thus propose a natural truncation of keeping just the $J' = 0$ terms and throwing away all the mixing terms $J' \neq 0$:

$$\begin{aligned} N(J, A, B, J', \rho) &\approx N(J, A, B, 0, \rho) \\ &= \frac{(J+1)^{\eta-1}}{(1+\rho^2)^{A+B+7J}} F_\rho^2(J) F_\rho^2\left(\frac{A+J}{2}\right) F_\rho^2\left(\frac{B+J}{2}\right). \end{aligned} \quad (85)$$

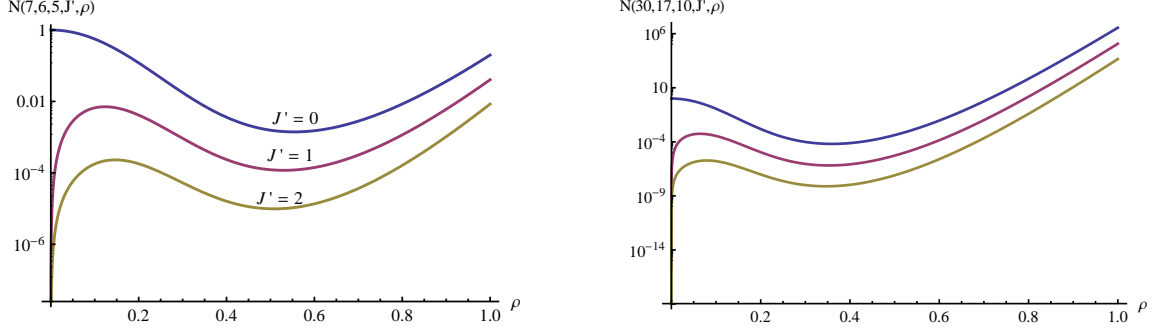


FIG. 23: Logarithmic plots for the coefficient N when $J = 7, A = 6, B = 5$, and $J = 30, A = 17, B = 10$. The blue, red, yellow lines correspond to $J' = 0, 1, 2$ respectively.

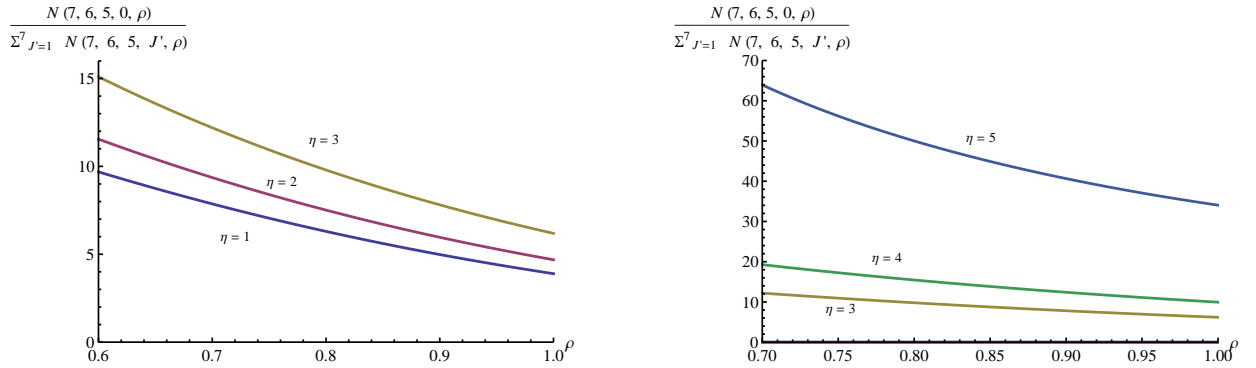


FIG. 24: Plots of the dependence of the ratio between $N(J' = 0)$ and the sum of subleading coefficients with face weight η when $J = 7, A = 6, B = 5$ and ρ is close to 1.

This truncation dramatically simplified the expression of N , making all the mixing and non-geometrical terms disappear. The truncation scheme can be graphically expressed as

$$\begin{array}{c} \text{Diagram of a vertex with four strands and a loop} \end{array} = \sum_{A,B,J} N(J' = 0) \begin{array}{c} \text{Diagram of a vertex with four strands} \end{array} + \sum_{A,B,J,J'} N(J' \neq 0) \begin{array}{c} \text{Diagram of a vertex with four strands and a loop} \end{array}. \quad (86)$$

Note that the left over strands will have to be integrated over in a calculation of a Spin Foam amplitude. And the contractions of these spinors give additional factors of $1/(1 + \rho^2)$, see the Appendix A. These factors will lead to additional suppression of amplitude for bigger ρ , making it more convergent. This however does not spoil the truncation. We will see the effect of this suppression in calculating the degree of divergence of Pachner moves in the coming section.

B. Counting the degree of divergence

Before we write out the truncated Pachner moves, let us first calculate how divergent the 5–1 move is as a function of face weight. The question of divergence is closely related to the one of symmetries. Indeed it is expected that in a physical model divergences of the partition function should be related to symmetries. This has been only shown exactly in 3 dimensions [65] so far.

In a model describing 4d gravity we would expect the 5–1 move to be invariant up to a divergence coming from the freedom of translation of the added vertex inside the 4-simplex. Hence we would

expect that for gravity the divergence should scale as $(length)^4$. Of course at this stage this is a naive guess but it would be harder to argue for a diffeomorphism symmetry otherwise. In the case of translational symmetry this divergence is due to the possibility of moving the internal vertex outside the geometrical simplex. It can be tamed by incorporating orientation dependent factors as shown in 3 dimensions [69]. The Spin Foam models at our disposal do not yet incorporate orientation dependence so it is unlikely that this phenomena can be used in our context.

The easiest way to count the degree of divergence is to set the external spins to 0, so that only the internal loops contribute. The calculation for the mixed 4 loops in the 5–1 move is rather involved, but thanks to the natural truncation discussed in the previous section we can do the calculation. Let us however first try to estimate the degree of divergence arising from a single loop in the 4–2 move. It is important to stress here that in this case we do not need to do the truncation, as setting the external spins to 0 corresponds to dropping all the products of spinors that contain the external ones in Eq. (79), and hence naturally makes all the mixing terms drop out⁵. This allows us to write the amplitude for the single loop in 4–2 move as

$$\mathcal{A}_\tau^{4-2}(0) = \int d\mu_\rho(w) e^{\frac{\tau_N^{AB} \tau_N^{AD} \tau_N^{BD} \tau'}{(1+\rho^2)^2}} \langle w|w \rangle = \frac{1}{\left(1 - \frac{\tau_N^{AB} \tau_N^{AD} \tau_N^{BD} \tau'}{(1+\rho^2)^3}\right)^2} = \sum_j (2j+1) \left(\frac{\tau_N^{AB} \tau_N^{AD} \tau_N^{BD} \tau'}{(1+\rho^2)^3} \right)^{2j}, \quad (87)$$

where, recall we have labeled the three loops, on which we applied the loop identity, by $\{AB, AD, BD\}$. Using the homogeneity map defined in Eq. (84), we can reintroduce the factors of face weight and the functions of ρ from loop identities. Regularizing the expression by putting a cut-off of Λ on spins, we get that a single loop in the 4–2 move is given by

$$D_{4-2}(\Lambda, \rho, \eta) = \sum_{j=0}^{\Lambda} \frac{(2j+1)^{4\eta-2}}{(1+\rho^2)^{24 \times 2j}} [{}_2F_1(-2j-1, -2j; 2; \rho^4)]^{12}. \quad (88)$$

It is easy to see that, since ${}_2F_1(-2j-1, -2j; 2; 0) = 1$, for $\rho = 0$ and $\eta = 1$ we recover the $SU(2)$ BF theory's divergence of a delta function $\delta_{SU(2)}(\mathbb{1})$. It may seem surprising that the exact result is this simple. For the purpose of analysing the divergence let us write $D_{4-2}(\Lambda, \rho, \eta) = \sum_{j=0}^{\Lambda} X_{4-2}(2j, \rho, \eta)$.

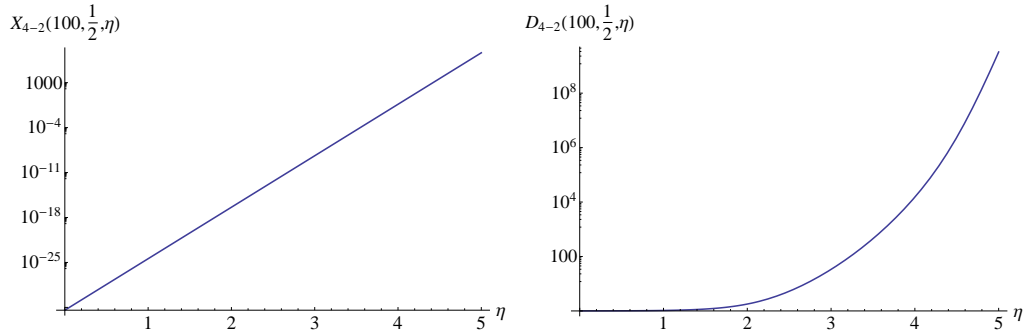


FIG. 25: X_{4-2} has an obvious dependence on η on a logarithmic plot. The sum diverges a lot faster with increasing η .

Let us start with analysing the behaviour of X_{4-2} and D_{4-2} as a function of η . This is shown in Fig. 25. Quite obviously, at fixed spin, both X_{4-2} and D_{4-2} are diverging with increasing η .

⁵ This is another reason for seeing that the mixing terms might not be important.

We get the opposite behaviour for increasing ρ – both X_{4-2} and D_{4-2} are heavily suppressed for increasing ρ , as can be seen in Fig. 26. This is the effect of the additional suppression by factors of $1/(1+\rho^2)$ that we mentioned in the previous section. We can thus expect interesting competition between ρ and η in concerning divergences.

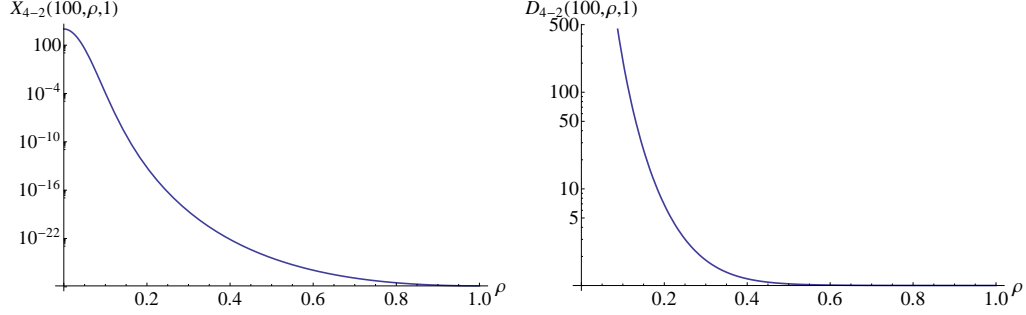


FIG. 26: X_{4-2} gets suppressed with increasing ρ , with $\rho = 0$ being the limit of SU(2) BF divergence. The sum is even more suppressed with increasing ρ .

Fixing ρ to a specific value, we can analyze now the divergence of X_{4-2} for different values of η , as a function of spin. We numerically find that X_{4-2} is suppressed with increasing spin, but at $\eta = 5$ there is a transition to divergence, see Fig. 27. This seems to be independent of the value of ρ , though the exact degree of divergence depends heavily on its value.

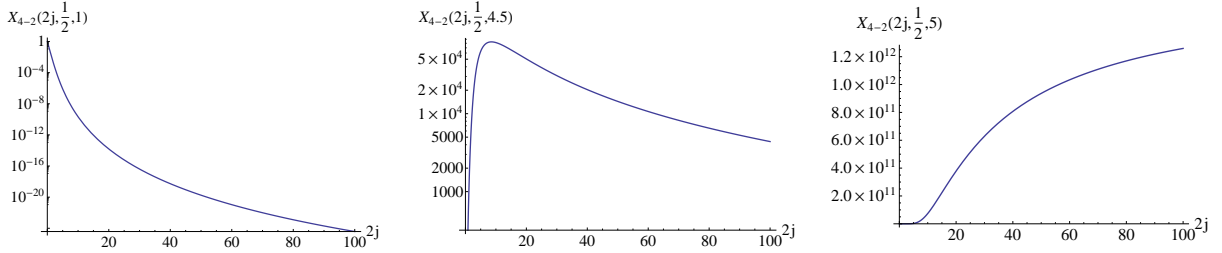


FIG. 27: For small values of η , X_{4-2} gets suppressed with increasing spin. There seems to be a transition in the behaviour for $\eta = 5$.

Let us now move onto the calculation of the degree of divergence for the 5–1 Pachner move. Truncating the loop identities in the 5–1 move allows us to perform the Gaussian integrals easily and write the four remaining loops as

$$\mathcal{A}_{\tau \text{ truncated}}^{5-1}(0) = \frac{1}{\left(1 + \frac{\tau_N^{AC} \tau_N^{AD} \tau_N^{CD} \tau'_y}{(1+\rho^2)^3}\right)^2 \left(1 + \frac{\tau_N^{AB} \tau_N^{AD} \tau_N^{BD} \tau'_b}{(1+\rho^2)^3}\right)^2 \left(1 + \frac{\tau_N^{AB} \tau_N^{AC} \tau_N^{BC} \tau'_g}{(1+\rho^2)^3}\right)^2 \left(1 + \frac{\tau_N^{BC} \tau_N^{BD} \tau_N^{CD} \tau'_r}{(1+\rho^2)^3}\right)^2}, \quad (89)$$

where, similarly as in the 4–2 move, the six loops that we have integrated out were labeled by the set $\{AB, AC, AD, BC, BD, CD\}$ and the left over four loops are labeled by $\{y, g, b, r\}$. Comparing this to the 4–2 move expression (87), we see that clearly we have 4 loops, that are not connected by any strands, but which are nonetheless coupled by sharing the τ s, and hence functions of spin and ρ . We can now expand this in a power series for the four spins j_y, j_g, j_b, j_r and reintroduce the factors of the hypergeometric functions and face weights by using the homogeneity map from Eq. (84). Letting $a, b, c \in \{y, g, b, r\}$ we can write the full expression for the degree of divergence

as

$$D_{5-1} = \sum_{j_y, j_p, j_b, j_r} \frac{\prod_a (2j_a + 1)^{\eta+1}}{(1+\rho^2)^{24 \sum_a 2j_a}} \left(\prod_{a < b} F_\rho(2j_a + 2j_b)^2 (2j_a + 2j_b + 1)^{\eta-1} \right) \left(\prod_{a < b < c} F_\rho(2j_a + 2j_b + 2j_c)^2 \right), \quad (90)$$

where, recall, we have previously defined $F_\rho(J) = {}_2F_1(-J-1, -J; 2; \rho^4)$ for simplification. Let us define $D_{5-1} = \sum_{\{j\}} X_{5-1}(j)$.

This general expression is rather long when expanded, but numerically it turns out that it is peaked around all the spins being equal. Hence for all spins equal to j , we have a nice simplification

$$X_{5-1}(\{j\}) = \frac{(2j+1)^{4(\eta+1)}(4j+1)^{6(\eta-1)}}{(1+\rho^2)^{96 \times 2j}} F_\rho(4j)^{12} F_\rho(6j)^8. \quad (91)$$

Again, it is easy to see that for $\rho = 0$ and $\eta = 1$ we recover the result of $\delta_{SU(2)}(\mathbb{1})^4$ for the SU(2) BF theory. We can now analyze the behaviour of X_{5-1} as a function of ρ . The results are qualitatively similar to those of 4-2 move, in the sense that the expression is suppressed for increasing ρ , see Fig. 28.

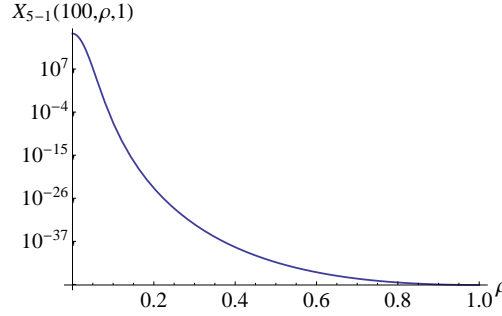


FIG. 28: X_{5-1} is suppressed with increasing ρ for all values of η and spin. This plot is evaluated at $2j = 100$ and $\eta = 1$.

Quite obviously X_{5-1} has similar behaviour to X_{4-2} as a function of η , so we will not present plots for this. The interesting difference is in the transition from convergence to divergence of each X_{5-1} term in the summation. The point of transition numerically seems to be around $\eta = 3.2$, see Fig. 29. Note, that the expression of D_{5-1} includes four summations, so it could become divergent

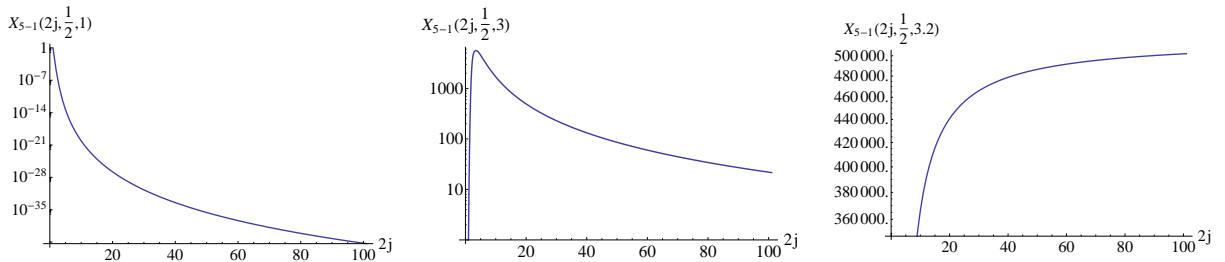


FIG. 29: For small values of η , X_{5-1} gets suppressed with increasing spin. There seems to be a transition in the behaviour for $\eta = 3.2$.

even before $\eta = 3.2$. We hence find that there is a range of the parameters (ρ, η) for which 4-2 Pachner move is finite and 5-1 move is divergent.

C. Truncated Pachner moves

Now that we have already studied their divergence properties, we can write down the full expression for the 4-dimensional Pachner moves after truncation of the loop identities. As we will see, even though the loops in the moves are no longer mixed, there is still non-local coupling by spins.

Let us start with the simple observation, that the truncation does not change the non-invariance of the 3–3 Pachner move. The loop inside does decouple, but the truncation of the constrained loop identity does not change the fact that the hypergeometric functions of ρ depend on different boundary spins in the two configurations. Thus even after the truncation, the 3–3 Pachner move is obviously not invariant, unless one considers very fine-tuned boundary spins.

Since the amplitude for the 4–2 and 5–1 moves look formally very similar, let us focus on the most interesting case of the 5–1 Pachner move. After truncation, the amplitude in Eq. (81) becomes

$$\begin{aligned} \mathcal{A}_{\tau \text{ truncated}}^{5-1}(z_{\gamma}^{\alpha f}) &= \int \prod_{\text{all}} d\mu_{\rho}(v, w) \prod_{\alpha} P_{\rho}(z_{\gamma}^{\alpha f}; w_{\gamma}^{\alpha f}) \cdot e^{\sum_{\sigma} \tilde{\tau}_{E\sigma} [\tilde{v}^{E\sigma} | \tilde{w}^{E\sigma}] + \sum_{\mu\kappa i} \tau_N^{\mu\nu} \beta_i^{\mu\nu} [v_i^{\mu\nu} | w_i^{\nu\mu}]} \\ &= \int \prod_{\text{left over}} d\mu_{\rho}(v, w) \prod_{\alpha} P_{\rho}(z_{\gamma}^{\alpha f}; w_{\gamma}^{\alpha f}) \cdot e^{\sum_{\sigma} \tilde{\tau}_{E\sigma} [\tilde{v}^{E\sigma} | \tilde{w}^{E\sigma}] + \sum_{\mu\nu} \tau_N^{\mu\nu} [v_f^{\mu\nu} | w_f^{\nu\mu}]} \mathcal{A}_{\tau \text{ truncated}}^{5-1}(0), \end{aligned} \quad (92)$$

where recall that indices run over $\sigma \in \{A, B, C, D\}$, $\mu\nu \in \{AB, AC, AD, BD, BC, CD\}$, $i \in \{f, b, r, y, g\}$, $\alpha, \gamma \in \{A, B, C, D, E\}$. We have also defined the amplitude with boundary spins set to zero, $\mathcal{A}_{\tau \text{ truncated}}^{5-1}(0)$, in the previous section in Eq. (89) to be given by

$$\mathcal{A}_{\tau \text{ truncated}}^{5-1}(0) = \frac{1}{\left(1 + \frac{\tau_N^{AC} \tau_N^{AD} \tau_N^{CD} \tau'_y}{(1+\rho^2)^3}\right)^2 \left(1 + \frac{\tau_N^{AB} \tau_N^{AD} \tau_N^{BD} \tau'_b}{(1+\rho^2)^3}\right)^2 \left(1 + \frac{\tau_N^{AB} \tau_N^{AC} \tau_N^{BC} \tau'_g}{(1+\rho^2)^3}\right)^2 \left(1 + \frac{\tau_N^{BC} \tau_N^{BD} \tau_N^{CD} \tau'_r}{(1+\rho^2)^3}\right)^2}.$$

It is imperative now to notice that this does not trivially factorize, as we still have to apply the homogeneity map to obtain the final expression. The map defined in Eq. (84) tells us that the τ_N s are actually functions of the $\tilde{\tau}$ s from the partially gauge-fixed propagators. The homogeneity map for the truncated 5–1 Pachner move is $H_{5-1}[\mathcal{A}_{\tau \text{ truncated}}^{5-1}] = \mathcal{A}_{\text{truncated}}^{5-1}$ and is given by

$$H_{5-1} : \tau_N^{\mu\nu J} \rightarrow F_{\rho}(J)^2 (J+1)^{\eta-1} \left(\frac{\tilde{\tau}_{E\mu} \tilde{\tau}_{E\nu}}{(1+\rho^2)^5} \right)^J, \quad \tilde{\tau}_{E\sigma}^J \rightarrow \frac{F_{\rho}(J/2)^2}{(1+\rho^2)^J}, \quad \tau_i'^{2j} \rightarrow (2j+1)^{\eta}. \quad (93)$$

Before applying this homogeneity map, we need to first integrate out the extra spinors on the internal strands – because of the previously inserted propagators, each strand now has two spinors, instead of one. This is a simple Gaussian integration that we have performed many times before. This however requires us to contract the boundary propagators P_{ρ} with functions of τ_N and $\tilde{\tau}$. We have to be careful now to perform these absorptions in a symmetric manner, which allow us after applying the homogeneity map (93) to define new boundary propagators \tilde{P}_{ρ} . The amplitude (92) is then expected to become

$$\mathcal{A}_{\text{truncated}}^{5-1}(z_{\gamma}^{\alpha f}) = \tilde{D}_{5-1} \int \prod_{\gamma} d\mu_{\rho}(w_{\gamma}) \prod_{\alpha} \tilde{P}_{\rho}(z_{\gamma}^{\alpha f}; w_{\gamma}^{\alpha f}). \quad (94)$$

This is the form of an amplitude for a 4-simplex with the modified propagators \tilde{P}_{ρ} weighted by an overall, possibly divergent, factor \tilde{D}_{5-1} which we expect, has the same degree of divergence as the function D_{5-1} we studied in the previous section. The exchange $P_{\rho} \rightarrow \tilde{P}_{\rho}$ now is a proposal for a

renormalization flow in the space of propagators (and perhaps the coefficient ρ and face weight as well). We leave the study of this flow and the behaviour of the other Pachner moves under it to future research.

VI. DISCUSSION

In this paper we have introduced a new Riemannian holomorphic Spin Foam model, with an alternative way of imposing holomorphic simplicity constraints. Instead of constraining the boundary spin network function, we impose the constraints on BF projectors. This model allows for more general graphs than the usual models built from vertex amplitudes. Surprisingly, it turns out to have the same asymptotics as the Dupuis-Livine model [57], and hence the same semi-classical limit as the seminal EPRL-FK model [60–62]. The holomorphic representation allows us to recast difficult integrals of $SU(2)$ Wigner D-matrices into much simpler spinor Gaussian integrals. This allows for exact evaluation of spin network functions in BF theory [24]. In our view the calculations done here realize the previously stated hope that the spinor formalism should allow the evaluation of expressions that could not be done in the standard language of group integrals. In this work we have defined a *homogeneity map*, which allowed us to extend these results to constrained models in the holomorphic representation, thus allowing us to evaluate all the Pachner moves in 3- and 4-dimensions explicitly.

In 3 dimensions, the results have been long known: the 3–2 move is invariant and 4–1 move is invariant up to a factor of an $SU(2)$ delta function, which results from not fixing the gauge translation symmetry. It is however the first time, that Pachner moves have been calculated explicitly in a simplicity-constrained Spin Foam model of 4-dimensional Quantum Gravity. The calculation of all the Pachner moves followed from a simplicity-constrained version of so-called *loop identity*. The crucial tool that allowed to find the constrained loop identity was the change from integrals over $SU(2)$ group elements to integrals over spinors and the use of the homogeneity map. We found that 4d gravity Spin Foam models are not invariant under 3–3 move unless very specific and symmetric boundary configurations are chosen. This is expected of a model for 4 dimensional gravity. A naive expectation, at least at the level of the classical action, is that the model should be invariant under the 4–2 and 5–1 Pachner moves. We found however this to be not the case for the exact evaluation. For both the 4–2 and 5–1 moves, there is an insertion of a non-local combination of $SU(N)$ grasping operators in the final coarse grained simplices, with a mixing of strands leading to non-geometrical and non-local configuration.

From the viewpoint of real-space renormalization group however, such non-local operators are expected to appear in each step of coarse graining, and have to be truncated to local ones in a controlled manner. Indeed, we have found that there exists a very accurate, natural and simple truncation scenario, which allows for a dramatic simplification of all of the 4-dimensional Pachner moves. Most crucially, the proposed truncation scheme removes the mixing of strands in the coarse-grained simplices, thus allowing them to remain geometrical, and hence making the 5–1 Pachner move structure preserving. After the truncation, the 4–2 and 5–1 Pachner moves are invariant up to a weight depending on the boundary spins. We should not expect an exact invariance, until a properly gauge-fixed model at a fixed point of renormalization flow corresponding to the continuum limit is found.

After introducing the truncation scheme, we have studied the divergence properties of the 4–2 and 5–1 moves. We find that the degree of divergence is crucially related to the two free parameters of the model – ρ (related to the Immirzi parameter) and the power of the face weight η . More precisely, we find that whether the moves are convergent or divergent depends on the choice of face weight η , but the exact scaling depends on ρ . The 4–2 Pachner moves transitions from convergence

to divergence for $\eta \geq 5$. The 5–1 move becomes divergent much faster – the transition is numerically evaluated to be around $\eta \geq 3.2$. As such, there is a range of parameters, for which 4–2 move is convergent, while 5–1 is divergent. The popular naive choice of $(2j+1)^2$ is then not in that range. However, the exact value of the parameters, at which 5–1 move is divergent depends probably on the exact normalization of the model considered, and as such might change under renormalization flow.

An important direction for future is to check whether the truncation scheme we have proposed is robust. As such, we should study other models and find whether removing the mixing of strands in the loop identity is a good approximation. This will be studied for the DL model in [70].

The next crucial step that we leave to future study is of course to analyze the renormalization of this constrained propagator model. It would be natural to renormalize both the coupling constants ρ and η , as well as the propagators $P_\rho(z_i; w_i)$. The evidence from renormalization of spin net models [39–41] seems to point to a very rich structure of fixed points in the renormalization flow for constrained spin foam models. Finding a fixed point invariant under 4–2 and 5–1 Pachner moves would give us a model invariant under discretized diffeomorphisms, and give hope to finding a continuum limit of the theory.

Acknowledgments

We would like to thank Bianca Dittrich, Aldo Riello and Lee Smolin for helpful discussions and comments on this work. Research at Perimeter Institute is supported by the Government of Canada through Industry Canada and by the Province of Ontario through the Ministry of Research and Innovation. This work is also part of the research program of the Foundation for Fundamental Research on Matter (FOM), all which is part of the Netherlands Organization for Scientific Research (NWO).

Appendix A: Gaussian Integration Techniques

In this appendix we compile a list of useful Gaussian spinor integrals. Consider first a standard Gaussian integral over the complex line \mathbb{C}

$$\int_{\mathbb{C}} \frac{d^2\alpha}{\pi^2} e^{-|\alpha|^2 + \bar{x}\alpha + y\bar{\alpha}} = e^{\bar{x}y}. \quad (\text{A1})$$

This easily generalizes to a Gaussian integration over spinors on \mathbb{C}^2 with the Bargmann measure $d\mu(z) = \pi^{-2} e^{-\langle z|z \rangle} d^4z$ giving us the integral that allows us to contract strands on cable graphs

$$\int_{\mathbb{C}^2} d\mu(z) e^{\langle x|z \rangle + \langle z|y \rangle} = e^{\langle x|y \rangle}. \quad (\text{A2})$$

It is interesting to note that this contraction also works with anti-holomorphic spinors $|z]$, since $[x|y] = \langle y|x \rangle$. We have thus

$$\int_{\mathbb{C}^2} d\mu(z) e^{\langle x|z \rangle + [z|y]} = e^{\langle x|y \rangle}. \quad (\text{A3})$$

As with usual Gaussian integrations, we can calculate Gaussian spinor integrals of arbitrary polynomials. The special case worth mentioning is of course how delta function acts on holomorphic functions

$$\int_{\mathbb{C}^2} d\mu(z) f(z) e^{\langle z|w \rangle} = f(w). \quad (\text{A4})$$

Let us now consider the integrals that are crucial to the computations in the paper – integrals with a matrix A . First consider the more familiar case of integrals over vectors of n complex numbers

$$\int_{\mathbb{C}^n} \prod_{i=1}^n \frac{d^2 \alpha_i}{\pi^2} e^{-\sum_{i,j} \bar{\alpha}_i A_{ij} \alpha_j} = \frac{1}{\det(A)} \quad (\text{A5})$$

This again trivially extends to the integrals over spinors. The expression useful for our paper is

$$\int_{\mathbb{C}^{2n}} \prod_{i=1}^n d\mu(z_i) e^{\sum_{i,j} \langle z_i | A_{ij} | z_j \rangle} = \frac{1}{\det(\mathbb{1} - A)}. \quad (\text{A6})$$

Recall that for the constrained model we had to change the measure of integration over spinors to $d\mu_\rho(z) = (1 + \rho^2)^2 \pi^{-2} e^{-(1+\rho^2)\langle z|z \rangle} d^4 z$. It is easy to check that this is normalized properly as

$$\int_{\mathbb{C}^2} \frac{(1 + \rho^2)^2 d^4 z}{\pi^2} e^{-(1+\rho^2)\langle z|z \rangle} = 1. \quad (\text{A7})$$

This change of measure leads to very simple changes to the above integrals. In particular, for a contraction we have

$$\int_{\mathbb{C}^2} d\mu_\rho(z) e^{\langle x|z \rangle + \langle z|y \rangle} = e^{(1+\rho^2)^{-1} \langle x|y \rangle}. \quad (\text{A8})$$

Hence for every contraction of spinors we pick up a factor of $1/(1 + \rho^2)$. Thus for a loop on which we have three spinors we get the factor of $(1 + \rho^2)^{-3}$ – this appears all the time in loop identity and Pachner moves calculations.

Appendix B: Mapping SU(2) to spinors

Lemma B.1. *Let $f \in L^2(\text{SU}(2))$ be homogeneous of degree $2J$, i.e. $f(\lambda g) = \lambda^{2J} f(g)$. Given a spinor by $|z\rangle$ define $g(z) = (|0\rangle\langle 0| + |0\rangle[0])g(z) = |0\rangle\langle z| + |0\rangle[z]$ where $|0\rangle = (1, 0)^t$. Then*

$$\int_{\mathbb{C}^2} d\mu(z) f(g(z)) = \Gamma(J + 2) \int_{\text{SU}(2)} dg f(g). \quad (\text{B1})$$

Proof. We can relate the inner product (6) to the standard $L^2(\text{SU}(2))$ inner product by parameterizing the spinor as

$$|z\rangle = \begin{pmatrix} r \cos \theta e^{i\phi} \\ r \sin \theta e^{i\psi} \end{pmatrix}, \quad (\text{B2})$$

where $r \in (0, \infty)$, $\theta \in [0, \pi/2)$, $\phi \in [0, 2\pi)$, $\psi \in [0, 2\pi)$. The Lebesgue measure in these coordinates is $d^4 z = r^3 \sin \theta \cos \theta dr d\phi d\theta d\psi$. Now using the homogeneity property $f(g(z)) = r^{2J} f(\tilde{g}(z))$ we have

$$\int_{\mathbb{C}^2} d\mu(z) f(g(z)) = \int_0^\infty dr r^{3+2J} e^{-r^2} \int_0^{\pi/2} d\theta \sin \theta \cos \theta \int_0^{2\pi} d\phi \int_0^{2\pi} d\psi f(\tilde{g}(z)), \quad (\text{B3})$$

where $\tilde{g}(z) \in \text{SU}(2)$. Performing the integral over r we get

$$\int dr r^{3+2J} e^{-r^2} = \frac{1}{2} \Gamma(J + 2) \quad (\text{B4})$$

and so

$$\int_{\mathbb{C}^2} d\mu(z) f(g(z)) = \Gamma(J + 2) \int_{\text{SU}(2)} dg f(g), \quad (\text{B5})$$

where dg is the normalized Haar measure on $\text{SU}(2)$. In our case J is an integer so $\Gamma(J + 2) = (J + 1)!$. \square

Appendix C: Group averaging the SU(2) projector

In this appendix we recall the calculation in [24] which shows that we can perform the integration over g explicitly for the BF projector (16), which we prove in the following theorem.

Theorem C.1. *The projector (16) can be expressed as a power series in the holomorphic spinor invariants as*

$$P(z_i; w_i) = \sum_{[k]} \frac{1}{(J+1)!} \prod_{i < j} \frac{([z_i|z_j][w_i|w_j])^{k_{ij}}}{k_{ij}!}. \quad (\text{C1})$$

where the sum is over sets of $n(n-1)/2$ non-negative integers k_{ij} with $1 \leq i < j \leq n$.

Proof. Expanding (16) in a power series

$$\int_{\text{SU}(2)} dg e^{[z_i|g|w_i]} = \sum_{j_i} \int dg \prod_i \frac{[z_i|g|w_i]^{2j_i}}{(2j_i)!}, \quad (\text{C2})$$

we see that each term in the sum is homogeneous of degree $2J = \sum_i (2j_i)$. This fact allows us to use Lemma B.1 detailed in Appendix B which says that we can replace the integral over SU(2) with a Gaussian integral paying a factor of $1/(J+1)!$ as in

$$(J+1)! \int dg \prod_i \frac{[z_i|g|w_i]^{2j_i}}{(2j_i)!} = \int d\mu(\alpha) \prod_i \frac{([z_i|0]\langle\alpha|w_i\rangle + [z_i|0][\alpha|w_i])^{2j_i}}{(2j_i)!}. \quad (\text{C3})$$

Now resum over j_i to get

$$\sum_{j_i} (J+1)! \int dg \prod_i \frac{[z_i|g|w_i]^{2j_i}}{(2j_i)!} = \int d\mu(\alpha) e^{\sum_i ([z_i|0]\langle\alpha|w_i\rangle + [z_i|0][\alpha|w_i])} = e^{\sum_{i,j} [z_i|0][0|z_j][w_i|w_j]}, \quad (\text{C4})$$

where we've performed the Gaussian integration in the second equality. Using the antisymmetry $[w_i|w_j] = -[w_j|w_i]$ and recognizing the identity $1 = |0\rangle\langle 0| + |0][0|$ in

$$\sum_{i,j} [z_i|0][0|z_j][w_i|w_j] = \sum_{i < j} [z_i(|0\rangle\langle 0| + |0][0|) |z_j\rangle [w_i|w_j] = \sum_{i < j} [z_j|z_i][w_i|w_j]. \quad (\text{C5})$$

Finally we have

$$\sum_{j_i} (J+1)! \int dg \prod_i \frac{[z_i|g|w_i]^{2j_i}}{(2j_i)!} = e^{\sum_{i < j} [z_j|z_i][w_i|w_j]} = \sum_{[k]} \prod_{i < j} \frac{([z_i|z_j][w_i|w_j])^{k_{ij}}}{k_{ij}!} \quad (\text{C6})$$

and since $J = \sum_{i < j} k_{ij}$ is just the total homogeneity of each term we can move the $(J+1)!$ to the RHS and complete the proof. \square

Appendix D: Proof of Lemma (III.2)

Proof. For a 2×2 matrix $2 \det M = \text{Tr}(M)^2 - \text{Tr}(M^2)$. If one consider $M = \mathbb{1} - \sum_i C_i |A_i\rangle [B_i|$, we have

$$\text{Tr}(M^2) = 2 - 2 \sum_i C_i [B_i|A_i] + \sum_{i,j} C_i C_j [B_i|A_j][B_j|A_i]$$

and

$$\text{Tr}(M)^2 = 4 - 4 \sum_i C_i [B_i | A_i] + \sum_{i,j} C_i C_j [B_i | A_i] [B_j | A_j],$$

therefore

$$2 \det(M) = 2 - 2 \sum_i C_i [B_i | A_i] + \sum_{i,j} C_i C_j ([B_i | A_i] [B_j | A_j] - [B_i | A_j] [B_j | A_i])$$

and using $[A_i | B_i] [B_j | A_j] - [A_i | B_j] [B_i | A_j] = [A_i | A_j] [B_j | B_i]$ gives the result. \square

Appendix E: Explicit calculation of the Constrained Loop Identity

In this appendix we explicitly show how to calculate the constrained loop identity (75). Let us consider the loop composed of two pairs of partially gauge-fixed propagators $\mathbb{1}_\rho \circ \mathbb{1}_\rho$ and one pair of propagators $P_\rho \circ P_\rho$. To calculate this loop, let us use the homogenized propagators $\mathbb{1}_{\tilde{\tau}} \circ \mathbb{1}_{\tilde{\tau}}$ and $G_\tau \circ G_\tau$ instead and at the end of the calculation use the homogeneity maps (73) and (74), which we recall are given by

$$\mathbb{1}_{\tilde{\tau}} \circ \mathbb{1}_{\tilde{\tau}} = e^{\tilde{\tau} \sum_i [\tilde{z}_i | \tilde{w}_i]} \quad \text{with} \quad \tilde{\tau}^J \rightarrow \frac{F_\rho(J/2)^2}{(1 + \rho^2)^J} \quad \text{for} \quad \mathbb{1}_{\tilde{\tau}} \circ \mathbb{1}_{\tilde{\tau}} \rightarrow \mathbb{1}_\rho \circ \mathbb{1}_\rho$$

for a pair of gauge-fixed propagators and by

$$G_\tau \circ G_\tau = e^{\tau \sum_{i < j} [z_i | z_j] [w_i | w_j]} \quad \text{with} \quad \tau^J \rightarrow \frac{F_\rho(J)^2}{(1 + \rho^2)^{2J} (J+1)!} \quad \text{for} \quad G_\tau \circ G_\tau \rightarrow P_\rho \circ P_\rho.$$

for the pair of propagators P_ρ . We will also insert a face weight by tracking the homogeneity of spin in the loop by a factor of τ' . The contractions of the spinors around the loop are as follows: $|w_4\rangle = |\tilde{w}_4^2\rangle$, $|\tilde{z}_4^2\rangle = |\tilde{z}_4^1\rangle$ and $|\tilde{w}_4^1\rangle = |z_4\rangle$. The cable diagram with all the labels is shown in Fig. 30.

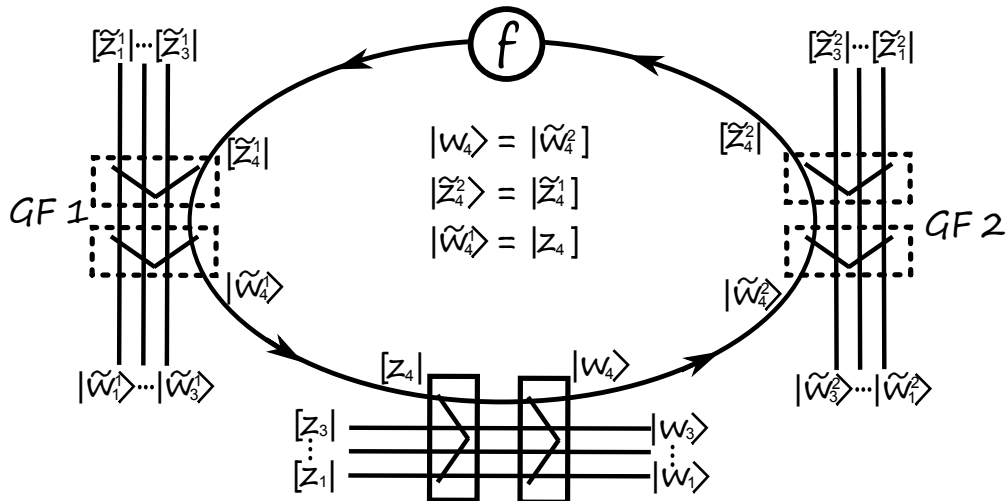


FIG. 30: Cable diagram with all the labels for the constrained loop identity.

We can thus finally calculate the loop identity:

$$\begin{aligned}
& \int d\mu_\rho(z_4, w_4, \tilde{z}_4^1) G_\tau^2(z_1, \dots, \tau' z_4; w_1, \dots, \tilde{w}_4^2) \mathbb{1}_{\tilde{\tau}_1}^2(\tilde{z}_1^1, \dots, \tilde{z}_4^1; \tilde{w}_1^1, \dots, \tilde{z}_4) \mathbb{1}_{\tilde{\tau}_2}^2(\tilde{z}_1^2, \dots, \tilde{z}_4^1; \tilde{w}_1^2, \dots, \tilde{w}_4^2) \\
&= \frac{e^{\tau \sum_{i<j<4} [z_i|z_j]\langle w_i|w_j\rangle + \sum_{i<4} \tilde{\tau}_1 [\tilde{z}_i^1|\tilde{w}_i^1] + \tilde{\tau}_2 [\tilde{z}_i^2|\tilde{w}_i^2]}}{1 - \frac{\tau \tilde{\tau}_1 \tilde{\tau}_2 \tau'}{(1+\rho^2)^3} \sum_{i<4} [z_i|w_i] + \left(\frac{\tau \tilde{\tau}_1 \tilde{\tau}_2 \tau'}{(1+\rho^2)^3}\right)^2 \sum_{i<j<4} [z_i|z_j]\langle w_i|w_j\rangle} \\
&= \exp \left(\tau \sum_{i<j<4} [z_i|z_j]\langle w_i|w_j\rangle + \sum_{i<4} \tilde{\tau}_1 [\tilde{z}_i^1|\tilde{w}_i^1] + \tilde{\tau}_2 [\tilde{z}_i^2|\tilde{w}_i^2] \right) \times \\
&\quad \times \sum_{N,M} \frac{(N+M)!}{N!M!} \left(\frac{\tau \tilde{\tau}_1 \tilde{\tau}_2 \tau'}{(1+\rho^2)^3} \right)^{N+2M} \left(\sum_{i<4} [z_i|w_i] \right)^N \left(- \sum_{i<j<4} [z_i|z_j]\langle w_i|w_j\rangle \right)^M.
\end{aligned}$$

The factor of $1/(1+\rho^2)^3$ arises from the three spinor integrations. Compared to the toy loop, the result is thus an exchange of $\frac{\tau\tau'}{1+\rho^2} \rightarrow \frac{\tau\tilde{\tau}_1\tilde{\tau}_2\tau'}{(1+\rho^2)^3}$ and the addition of the trivial propagation of the gauge-fixed strands. Before we can use the homogeneity maps we have to expand the exponentials in a power series. Doing this we arrive at

$$\begin{aligned}
& \sum_{A,B,C,M,N} \frac{(-1)^M (N+M)!}{A!B!C!M!N!} \left(\frac{\tau \tilde{\tau}_1 \tilde{\tau}_2 \tau'}{(1+\rho^2)^3} \right)^{N+2M} \tilde{\tau}_1^A \tilde{\tau}_2^B \tau^C \times \\
& \times \left(\sum_{i<4} [\tilde{z}_i^1|\tilde{w}_i^1] \right)^A \left(\sum_{i<4} [\tilde{z}_i^2|\tilde{w}_i^2] \right)^B \left(\sum_{i<4} [z_i|w_i] \right)^N \left(\sum_{i<j<4} [z_i|z_j]\langle w_i|w_j\rangle \right)^{M+C}.
\end{aligned}$$

Relabeling $N \rightarrow J$ and $M+C \rightarrow J'$ and using the above homogeneity maps for $\tau, \tilde{\tau}_1, \tilde{\tau}_2$ and $\tau'^{2j} \rightarrow (2j+1)^\eta$, we recover the result for the constrained loop identity (75).

-
- [1] C. Rovelli, “Zakopane lectures on loop gravity,” PoS QGQS **2011**, 003 (2011) [arXiv:1102.3660 [gr-qc]].
 - [2] A. Perez, “The Spin Foam Approach to Quantum Gravity,” Living Rev. Rel. **16**, 3 (2013) [arXiv:1205.2019 [gr-qc]].
 - [3] B. Bahr, “On background-independent renormalization of spin foam models,” arXiv:1407.7746 [gr-qc].
 - [4] D. Mamone and C. Rovelli, “Second-order amplitudes in loop quantum gravity,” Class. Quant. Grav. **26**, 245013 (2009) [arXiv:0904.3730 [gr-qc]].
 - [5] A. Riello, “Self-energy of the Lorentzian Engle-Pereira-Rovelli-Livine and Freidel-Krasnov model of quantum gravity,” Phys. Rev. D **88**, no. 2, 024011 (2013) [arXiv:1302.1781 [gr-qc]].
 - [6] B. Dittrich, S. Mizera and S. Steinhaus, “Decorated tensor network renormalization for lattice gauge theories and spin foam models,” arXiv:1409.2407 [gr-qc].
 - [7] J. F. Plebanski, “On the separation of Einsteinian substructures,” J. Math. Phys. **18**, 2511 (1977).
 - [8] L. Freidel and K. Krasnov, “A New Spin Foam Model for 4d Gravity,” Class. Quant. Grav. **25**, 125018 (2008) [arXiv:0708.1595 [gr-qc]].
 - [9] J. Engle, R. Pereira and C. Rovelli, “The Loop-quantum-gravity vertex-amplitude,” Phys. Rev. Lett. **99**, 161301 (2007) [arXiv:0705.2388 [gr-qc]].
 - [10] J. Engle, R. Pereira and C. Rovelli, “Flipped spinfoam vertex and loop gravity,” Nucl. Phys. B **798**, 251 (2008) [arXiv:0708.1236 [gr-qc]].
 - [11] J. Engle, E. Livine, R. Pereira and C. Rovelli, “LQG vertex with finite Immirzi parameter,” Nucl. Phys. B **799**, 136 (2008) [arXiv:0711.0146 [gr-qc]].
 - [12] M. Dupuis and E. R. Livine, “Holomorphic Simplicity Constraints for 4d Spinfoam Models,” Class. Quant. Grav. **28**, 215022 (2011) [arXiv:1104.3683 [gr-qc]].

- [13] E.R. Livine and S. Speziale, “A new spinfoam vertex for quantum gravity”, *Phys.Rev.D* **76** (2007) 084028 [arXiv:0705.0674]
- [14] E. R. Livine and S. Speziale, “Consistently Solving the Simplicity Constraints for Spinfoam Quantum Gravity,” *Europhys. Lett.* **81**, 50004 (2008) [arXiv:0708.1915 [gr-qc]].
- [15] L. Freidel, K. Krasnov and E. R. Livine, “Holomorphic Factorization for a Quantum Tetrahedron,” *Commun. Math. Phys.* **297**, 45 (2010) [arXiv:0905.3627 [hep-th]].
- [16] L. Freidel and E. R. Livine, “The Fine Structure of $SU(2)$ Intertwiners from $U(N)$ Representations,” *J. Math. Phys.* **51**, 082502 (2010) [arXiv:0911.3553 [gr-qc]].
- [17] L. Freidel and E. R. Livine, “ $U(N)$ Coherent States for Loop Quantum Gravity,” *J. Math. Phys.* **52**, 052502 (2011) [arXiv:1005.2090 [gr-qc]].
- [18] E. F. Borja, L. Freidel, I. Garay and E. R. Livine, “ $U(N)$ tools for Loop Quantum Gravity: The Return of the Spinor,” *Class. Quant. Grav.* **28**, 055005 (2011) [arXiv:1010.5451 [gr-qc]].
- [19] E. R. Livine and J. Tambornino, “Spinor Representation for Loop Quantum Gravity,” *J. Math. Phys.* **53**, 012503 (2012) [arXiv:1105.3385 [gr-qc]].
- [20] M. Dupuis, S. Speziale and J. Tambornino, “Spinors and Twistors in Loop Gravity and Spin Foams,” *PoS QGQGS* **2011**, 021 (2011) [arXiv:1201.2120 [gr-qc]].
- [21] M. Dupuis and E. R. Livine, “Revisiting the Simplicity Constraints and Coherent Intertwiners,” *Class. Quant. Grav.* **28**, 085001 (2011) [arXiv:1006.5666 [gr-qc]].
- [22] M. Dupuis and E. R. Livine, “Holomorphic Simplicity Constraints for 4d Riemannian Spinfoam Models,” *J. Phys. Conf. Ser.* **360**, 012046 (2012) [arXiv:1111.1125 [gr-qc]].
- [23] M. Dupuis, L. Freidel, E. R. Livine and S. Speziale, “Holomorphic Lorentzian Simplicity Constraints,” *J. Math. Phys.* **53**, 032502 (2012) [arXiv:1107.5274 [gr-qc]].
- [24] L. Freidel and J. Hnybida, “On the exact evaluation of spin networks,” arXiv:1201.3613 [gr-qc].
- [25] I. Montvay and G. Münster, “Quantum fields on a lattice,” Cambridge, UK: Univ. Pr. (1994) 491 p. (Cambridge monographs on mathematical physics)
- [26] F. Markopoulou, “Coarse graining in spin foam models,” *Class. Quant. Grav.* **20**, 777 (2003) [gr-qc/0203036].
- [27] R. Oeckl, “Renormalization of discrete models without background,” *Nucl. Phys. B* **657**, 107 (2003) [gr-qc/0212047].
- [28] R. Oeckl, “Renormalization for spin foam models of quantum gravity,” In *Rio de Janeiro 2003, Recent developments in theoretical and experimental general relativity, gravitation, and relativistic field theories, pt. C* 2296-2300 [gr-qc/0401087].
- [29] A. Ashtekar and J. Lewandowski, “Projective techniques and functional integration for gauge theories,” *J. Math. Phys.* **36**, 2170 (1995) [gr-qc/9411046].
- [30] A. Ashtekar and J. Lewandowski, “Differential geometry on the space of connections via graphs and projective limits,” *J. Geom. Phys.* **17**, 191 (1995) [hep-th/9412073].
- [31] A. Baratin, B. Dittrich, D. Oriti and J. Tambornino, “Non-commutative flux representation for loop quantum gravity,” *Class. Quant. Grav.* **28**, 175011 (2011) [arXiv:1004.3450 [hep-th]].
- [32] B. Dittrich, “From the discrete to the continuous: Towards a cylindrically consistent dynamics,” *New J. Phys.* **14**, 123004 (2012) [arXiv:1205.6127 [gr-qc]].
- [33] M. Levin, C. P. Nave, “Tensor renormalization group approach to 2D classical lattice models,” *Phys. Rev. Lett.* **99** (2007) 120601.
- [34] S. Singh and G. Vidal, “Tensor network states and algorithms in the presence of a global $SU(2)$ symmetry,” *Phys. Rev. B* **86**, 195114 (2012) [arXiv:1208.3919 [cond-mat.str-el]].
- [35] Z. C. Gu and X. G. Wen, “Tensor-Entanglement-Filtering Renormalization Approach and Symmetry Protected Topological Order,” *Phys. Rev. B* **80**, 155131 (2009) [arXiv:0903.1069 [cond-mat.str-el]].
- [36] B. Dittrich, F. C. Eckert and M. Martin-Benito, “Coarse graining methods for spin net and spin foam models,” *New J. Phys.* **14**, 035008 (2012) [arXiv:1109.4927 [gr-qc]].
- [37] B. Dittrich and F. C. Eckert, “Towards computational insights into the large-scale structure of spin foams,” *J. Phys. Conf. Ser.* **360**, 012004 (2012) [arXiv:1111.0967 [gr-qc]].
- [38] B. Bahr, B. Dittrich, F. Hellmann and W. Kaminski, “Holonomy Spin Foam Models: Definition and Coarse Graining,” *Phys. Rev. D* **87**, 044048 (2013) [arXiv:1208.3388 [gr-qc]].
- [39] B. Dittrich, M. Martin-Benito and E. Schnetter, “Coarse graining of spin net models: dynamics of intertwiners,” *New J. Phys.* **15**, 103004 (2013) [arXiv:1306.2987 [gr-qc]].
- [40] B. Dittrich and W. Kaminski, “Topological lattice field theories from intertwiner dynamics,”

- arXiv:1311.1798 [gr-qc].
- [41] B. Dittrich, M. Martin-Benito and S. Steinhaus, “Quantum group spin nets: refinement limit and relation to spin foams,” *Phys. Rev. D* **90**, 024058 (2014) [arXiv:1312.0905 [gr-qc]].
 - [42] E. R. Livine and D. Oriti, “Coupling of spacetime atoms and spin foam renormalisation from group field theory,” *JHEP* **0702**, 092 (2007) [gr-qc/0512002].
 - [43] L. Freidel, R. Gurau and D. Oriti, “Group field theory renormalization - the 3d case: Power counting of divergences,” *Phys. Rev. D* **80**, 044007 (2009) [arXiv:0905.3772 [hep-th]].
 - [44] J. Ben Geloun and V. Rivasseau, “A Renormalizable 4-Dimensional Tensor Field Theory,” *Commun. Math. Phys.* **318**, 69 (2013) [arXiv:1111.4997 [hep-th]].
 - [45] V. Rivasseau, “Quantum Gravity and Renormalization: The Tensor Track,” *AIP Conf. Proc.* **1444**, 18 (2011) [arXiv:1112.5104 [hep-th]].
 - [46] J. Ben Geloun and D. O. Samary, “3D Tensor Field Theory: Renormalization and One-loop β -functions,” *Annales Henri Poincaré* **14**, 1599 (2013) [arXiv:1201.0176 [hep-th]].
 - [47] J. Ben Geloun and E. R. Livine, “Some classes of renormalizable tensor models,” *J. Math. Phys.* **54**, 082303 (2013) [arXiv:1207.0416 [hep-th]].
 - [48] S. Carrozza, D. Oriti and V. Rivasseau, “Renormalization of Tensorial Group Field Theories: Abelian $U(1)$ Models in Four Dimensions,” *Commun. Math. Phys.* **327**, 603 (2014) [arXiv:1207.6734 [hep-th]].
 - [49] D. O. Samary and F. Vignes-Tourneret, “Just Renormalizable TGFT’s on $U(1)^d$ with Gauge Invariance,” *Commun. Math. Phys.* **329**, 545 (2014) [arXiv:1211.2618 [hep-th]].
 - [50] S. Carrozza, D. Oriti and V. Rivasseau, “Renormalization of a $SU(2)$ Tensorial Group Field Theory in Three Dimensions,” *Commun. Math. Phys.* **330**, 581 (2014) [arXiv:1303.6772 [hep-th]].
 - [51] J. Ben Geloun, “Renormalizable Models in Rank $d \geq 2$ Tensorial Group Field Theory,” arXiv:1306.1201 [hep-th].
 - [52] S. Carrozza, “Discrete Renormalization Group for $SU(2)$ Tensorial Group Field Theory,” arXiv:1407.4615 [hep-th].
 - [53] U. Pachner, “P.L. homeomorphic manifolds are equivalent by elementary shellings,” *European Journal of Combinatorics* **12** (2), 129145 (1991)
 - [54] B. Dittrich and S. Steinhaus, “Path integral measure and triangulation independence in discrete gravity,” *Phys. Rev. D* **85**, 044032 (2012) [arXiv:1110.6866 [gr-qc]].
 - [55] C. Perini, C. Rovelli and S. Speziale, “Self-energy and vertex radiative corrections in LQG,” *Phys. Lett. B* **682**, 78 (2009) [arXiv:0810.1714 [gr-qc]].
 - [56] B. Dittrich, W. Kaminski and S. Steinhaus, “Discretization independence implies non-locality in 4D discrete quantum gravity,” arXiv:1404.5288 [gr-qc].
 - [57] A. Banburski, L. Q. Chen, L. Freidel and J. Hnybida, “Spin foam factory,” in preparation.
 - [58] V. Bargmann, “On the Representations of the Rotation Group,” *Rev. Mod. Phys.* **34**, 829 (1962).
 - [59] J. Schwinger, “On Angular Momentum,” U.S. Atomic Energy Commission. (unpublished) NYO-3071, (1952).
 - [60] F. Conrady and L. Freidel, “On the semiclassical limit of 4d spin foam models,” *Phys. Rev. D* **78**, 104023 (2008) [arXiv:0809.2280 [gr-qc]].
 - [61] J. W. Barrett, R. J. Dowdall, W. J. Fairbairn, H. Gomes and F. Hellmann, “Asymptotic analysis of the EPRL four-simplex amplitude,” *J. Math. Phys.* **50**, 112504 (2009) [arXiv:0902.1170 [gr-qc]].
 - [62] M. X. Han and M. Zhang, “Asymptotics of Spinfoam Amplitude on Simplicial Manifold: Euclidean Theory,” *Class. Quant. Grav.* **29**, 165004 (2012) [arXiv:1109.0500 [gr-qc]].
 - [63] T. Regge, “General Relativity Without Coordinates,” *Nuovo Cim.* **19**, 558 (1961).
 - [64] L. Freidel and J. Hnybida, “A Discrete and Coherent Basis of Intertwiners,” arXiv:1305.3326 [math-ph].
 - [65] L. Freidel and D. Louapre, “Diffeomorphisms and spin foam models,” *Nucl. Phys. B* **662**, 279 (2003) [gr-qc/0212001].
 - [66] L. Freidel and E. R. Livine, “Spin networks for noncompact groups,” *J. Math. Phys.* **44**, 1322 (2003) [hep-th/0205268].
 - [67] L. Freidel and K. Krasnov, *Adv. Theor. Math. Phys.* **2**, 1183 (1999) [hep-th/9807092].
 - [68] E. R. Livine and J. Tambornino, “Holonomy Operator and Quantization Ambiguities on Spinor Space,” *Phys. Rev. D* **87**, no. 10, 104014 (2013) [arXiv:1302.7142 [gr-qc]].
 - [69] M. Christodoulou, M. Langvik, A. Riello, C. Roken and C. Rovelli, *Class. Quantum Grav.* **30**, 055009 (2013) [arXiv:1207.5156 [gr-qc]].
 - [70] A. Banburski, L. Q. Chen, “Pachner moves in the DL model” in preparation.

- [71] L. Freidel and D. Louapre, “Ponzano-Regge model revisited II: Equivalence with Chern-Simons,” gr-qc/0410141.
- [72] J. W. Barrett and I. Naish-Guzman, “The Ponzano-Regge model and Reidemeister torsion,” gr-qc/0612170.
- [73] V. Bonzom and M. Smerlak, “Bubble divergences from cellular cohomology,” Lett. Math. Phys. **93**, 295 (2010) [arXiv:1004.5196 [gr-qc]].
- [74] V. Bonzom and M. Smerlak, “Bubble divergences: sorting out topology from cell structure,” Annales Henri Poincare **13**, 185 (2012) [arXiv:1103.3961 [gr-qc]].